# The serotonin 2B receptor is required in neonatal microglia to limit neuroinflammation and sickness behavior in adulthood

Catherine Béchade, Ivana d'Andrea, Fanny Etienne, Franck Verdonk, Imane Moutkine, Sophie M Banas, Marta Kolodziejczak, Silvina Diaz, Christopher Parkhurst, Wenbiao Gan, et al.

**The serotonin 2B receptor is required in neonatal microglia to limit neuroinflammation and sickness behavior in adulthood.**

**Short/running title:** Microglia, 5-HT and neuroinflammation

Béchade, C[1,2,3], D'Andrea, I[1,2,3,*], Etienne, F[1,2,3,*], Verdonk, F[4,7], Moutkine, I[1,2,3], Banas, SM[1,2,3], Kolodziejczak, M[1,2,3,8], Diaz, SL[1,2,3,5], Parkhurst, CN[6,9], Gan W-B[6], Maroteaux, L[1,2,3], Roumier, A[1,2,3]

[1]INSERM UMR-S 1270, F-75005, Paris, France

[2]Sorbonne Université, Faculté des Sciences et Ingénierie, F-75005, Paris

[3]Institut du Fer à Moulin, F-75005, Paris

[4]Experimental Neuropathology, Infection and Epidemiology Department, Institut Pasteur, Paris, France

[5]current address: Instituto de Biología Celular y Neurociencia, UBA-CONICET – Paraguay 2155, 3º piso, C1121ABG Buenos Aires, Argentina

[6]Molecular Neurobiology Program, The Kimmel Center for Biology and Medicine at the Skirball Institute, Department of Neuroscience and Physiology, New York University School of Medicine, New York, NY 10016, USA;

[7]current address: Stanford University, School of Medicine, Stanford, CA 93304, USA

[8]current address: Ludwig-Maximilians University Munich, Dep. of Metabolic Biochemistry, 81377 Munich, Germany

[9]current address: Weill Cornell Medicine, New York, NY 10065, USA.

[*] equal contribution

· **Corresponding author's complete mailing address, phone, and email**

Anne Roumier: Sorbonne Université - INSERM UMR-S1270, 17 rue du Fer à Moulin, Paris, 75005, France ; Phone 33 1 45 87 61 27 ; Email: anne.roumier@inserm.fr

***Fundings***

This work has been supported by grants from the French Ministry of Research (*Agence Nationale pour la Recherche* ANR-17-CE16-0008 and the *Investissements d'Avenir* program ANR-11-IDEX-0004-02), the *Fondation pour la Recherche Médicale* "Equipe FRM DEQ2014039529", the *Fondation pour la Recherche sur le Cerveau*, the *Fondation de France* and the Emergence program 2011/2014 of *Sorbonne Université*, and by funds from the *Institut National de la Santé et de la Recherche Médicale*, *Sorbonne Université* and the *Centre National de la Recherche Scientifique*. The cytometry equipments have been acquired with the support of the *DIM Cerveau et Pensée -Région Ile-de-France* (PME 2012, Neurocytometrie project) and of the *Bio-Psy Labex* (ANR-11-IDEX-0004-02). LM is part of the *École des Neurosciences de Paris Ile-de-France* network.

***Acknowledgment***

We thank Giulia Albertini and Patricia Gaspar for the fruitful discussions and suggestions; the *Cell and Tissue Imaging Facility* of the Institut du Fer à Moulin (namely Theano Eirinopoulou and Mythili Savariradjane), where all image acquisitions and analyses have been performed; François Baudoin and Gaël Grannec at the IFM animal facility; the students Ezequiel Aranda, Damien Blot, Elodie Stievenard, Rayhan Haddad.

***Authorship***

CB designed, conducted and analyzed experiments and wrote the paper; IDA, FE and MK conducted and analyzed experiments and corrected the paper; FV, IM, SMB and SLD conducted and analyzed experiments; CNP and WBG provided reagents and corrected the paper; LM supervised the project, analyzed experiments, provided funding and wrote the paper; AR supervised the project, designed, conducted and analyzed experiments, provided funding and wrote the paper.

***Conflicts of interest:***

None

***Data Availability Statement:***

The data that support the findings of this study are available from the corresponding author upon reasonable request.

**· Word count of the abstract: 248**
**· Word count of the main text: 4756**
**· Number of figures, 5 Tables, 0 Supplemental information, 1 (8 Sup Fig and 2 sup Tables)**
**· Keywords:**
Neuroinflammation; microglia; serotonin; sickness syndrome; 5-$HT_{2B}$ receptor; LPS


***Abstract***

Severe peripheral infections induce an adaptive sickness behavior and an innate immune reaction in various organs including the brain. On the long term, persistent alteration of microglia, the brain innate immune cells, is associated with an increased risk of psychiatric disorders. It is thus critical to identify genes and mechanisms controlling the intensity and duration of the neuroinflammation induced by peripheral immune challenges. We tested the hypothesis that the 5-$HT_{2B}$ receptor, the main serotonin receptor expressed by microglia, might represent a valuable candidate. First, we observed that *Htr2b*$^{-/-}$ mice, knock-out for the 5-$HT_{2B}$ receptor gene, developed, when exposed to a peripheral lipopolysaccharide (LPS) challenge, a stronger weight loss compared to wild-type mice; in addition, comparison of inflammatory markers in brain, 4 and 24 hours after LPS injection, showed that *Htr2b* deficiency leads to a prolonged neuroinflammation. Second, to assess the specific contribution of the microglial 5-$HT_{2B}$ receptor, we investigated the response to LPS of conditional knock-out mice invalidated for *Htr2b* in microglia only. We found that deletion of *Htr2b* in microglia since birth is sufficient to cause enhanced weight loss and increased neuroinflammatory response upon LPS injection at adult stage. In contrast, mice deleted for microglial *Htr2b* in adulthood responded normally to LPS, revealing a neonatal developmental effect. These results highlight the role of microglia in the response to a peripheral immune challenge and suggest the existence of a developmental, neonatal period, during which instruction of microglia through 5-$HT_{2B}$ receptors is necessary to prevent microglia overreactivity in adulthood.


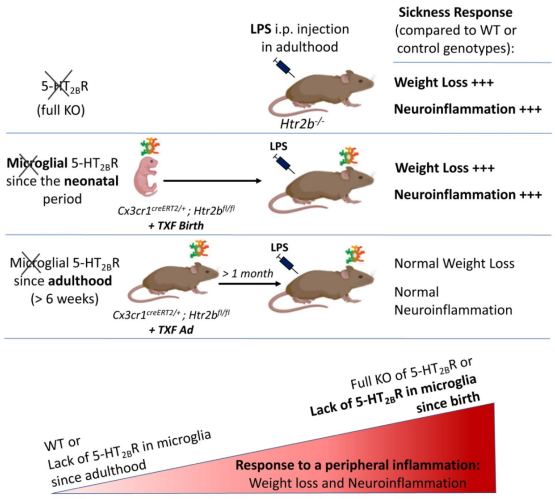


***Main points***

- Lack of 5-$HT_{2B}$ receptor in microglia since birth sensitizes to the neuroinflammation induced by a peripheral LPS injection in adulthood
- This effect is not observed if the gene is invalidated in adulthood, suggesting a neonatal critical period for instruction of microglia by 5-HT

***Introduction***

Peripheral inflammation induces a sickness behavior characterized by anhedonia, anorexia, weight loss, decreased locomotion and reduction of social interactions. Peripheral immune responses impact on brain and thus behavior through the vagus nerve and circulating signals, which may modulate neurons either directly or indirectly, through activation of other cells including microglia (Dantzer et al., 2008; Hoogland et al., 2015; Norden et al., 2016; Rivest, 2009). Sickness behavior is generally considered to be adaptive, but can be harmful when prolonged (Cunningham, 2013). In addition, persistent residual neuroinflammation and microglial activation have been associated with numerous brain disorders (Perry & Holmes, 2014; Tay et al., 2018). To prevent the negative impacts of peripheral immune challenges, it is thus important to identify genes, cells and pathways controlling the severity of sickness behavior and of neuroinflammation.

Among the candidates is the serotonin (5-Hydroxytryptamine, 5-HT) pathway, which is at the interface between the immune and the central nervous systems (Baganz & Blakely, 2013). Notably, the *Htr2b* gene, which encodes the 5-$HT_{2B}$ receptor, is expressed in microglia (Kolodziejczak et al., 2015; Krabbe et al., 2012) and in subsets of serotonin (Diaz et al., 2012) and dopamine (Doly et al., 2017) neurons. Absence or decreased expression of this gene is correlated with impulsivity in mice and humans (Bevilacqua et al., 2010; Montalvo-Ortiz et al., 2018), and with hyperactivity, sleep disturbance (Pitychoutis et al., 2015) and resistance to selective serotonin recapture inhibitors (SSRI) (Diaz et al., 2012) in mice. Moreover, in a mouse model of amyotrophic lateral sclerosis, a neurodegenerative disease involving the immune system, loss of *Htr2b* is associated with an acceleration of disease progression (El Oussini et al., 2016). The cell types involved in these various phenotypes are not identified yet but, in murine primary cultures of microglia, a lack of *Htr2b* expression results in overexpression of several cytokine receptors genes in basal conditions (Kolodziejczak et al., 2015). In addition, the 5-$HT_{2B}$ receptor mediates the effect of serotonin on human peripheral macrophages polarization toward an anti-inflammatory state (de Las Casas-Engel et al., 2013; Szabo et al., 2018). Altogether, this suggests a role of 5-$HT_{2B}$ receptor in controlling microglial activation and differentiation. We thus postulated that the *Htr2b* gene might participate to sickness behavior and neuroinflammation induced by a peripheral immune challenge, through a regulatory effect on microglia.

To test this hypothesis, we first compared, in wild-type and 5-$HT_{2B}$-receptor full knock-out ($Htr2b^{-/-}$) mice, the behavioral and neuroinflammatory effects of an intraperitoneal injection of bacterial wall Lipopolysaccharide (LPS), a reliable model of peripheral immune challenge. To analyze the specific contribution of the microglial 5-$HT_{2B}$ receptor, we then replicated these experiments in conditional knock-out mice deleted for this gene in microglia only ($Cx3cr1^{creERT2/+}$; $Htr2b^{fl/fl}$ mice). Our conclusions are that 1) the lack of the *Htr2b* gene sensitizes to weight loss, microglial reaction, and neuroinflammation induced by a peripheral injection of LPS, with several cytokines remaining abnormally elevated in the brain 24h after the immune challenge; 2) the specific invalidation of *Htr2b* in microglia since the neonatal stage is sufficient to exacerbate the effect of LPS; 3) on the contrary, invalidation of microglial *Htr2b* in adulthood does not affect the response to LPS, pointing out a developmental role of the microglial 5-$HT_{2B}$ receptor. Thereby, our results identify *Htr2b* as a susceptibility gene for exacerbated weight loss and neuroinflammation, due to its expression in microglia, and suggest that instruction of microglia through 5-$HT_{2B}$ receptor during a critical neonatal period is required to limit microglia responsiveness in adulthood.

***Methods and Materials (1796 words)***

**Animals**

*Htr2b*$^{-/-}$ knock-out mice (*129S2.Cg-Htr2b*$^{tm1Lum}$*/Htr2b*$^{tm1Lum}$*)* were generated and maintained on the 129S2/SvPas (referred to as 129S2 hereafter) background (Nebigil et al., 2000). Wild-type 129S2 mice were used as control. *Htr2b*$^{fl/fl}$**,** the *Htr2b* floxed mice (*Htr2b*$^{tm2Lum}$*/Htr2b*$^{tm2Lum}$), were generated as described (Belmer et al., 2018; Doly et al., 2017) with backcrossing on 129S2 background for >10 generations. *Cx3cr1*$^{CreERT2}$ knock-in mice, which express tamoxifen-inducible Cre recombinase in microglia under the control of the endogenous *Cx3cr1* promoter, have been previously described (Parkhurst et al., 2013) and were backcrossed on 129S2 background (with *Htr2b*$^{fl/fl}$ mice) for >10 generations. Along the procedure, only *Cx3cr1*$^{CreERT2/+}$ males were used for breeding. *Cx3cr1*$^{CreERT2/+}$; *Htr2b*$^{fl/fl}$ were compared to *Cx3cr1*$^{+/+}$; *Htr2b*$^{fl/fl}$ littermates. *Cx3cr1*$^{GFP}$ mice (Jung et al., 2000), used for flow cytometry and cell morphology analyses were backcrossed on 129S2 background for >10 generations and the line was crossed with *Htr2b*$^{-/-}$ to obtain *Cx3cr1*$^{GFP/+}$*; Htr2b*$^{-/-}$ mice.

Temperature was maintained at 21±1°C, under 12/12h light/dark. All mice were bred in our animal facility. Food and water were available *ad libitum.* Mice were moved to the experimental room in their home cage at least 5 days prior to testing to allow for habituation to the environment. All experiments involving mice were conducted in accordance with the standard ethical guidelines (National Institutes of Health's 'Guide for the care and use of Laboratory animals' and European Directive 2010/63/ UE) and approved by our local ethical committee (Darwin Committee, agreements #1170 and #10921).

**Tamoxifen treatment**

Cre-mediated recombination in neonates and adults was induced as in (Parkhurst et al., 2013). Briefly, neonatal recombination ("invalidation at birth", **Fig. 4B-G, S7, and S8A**) was induced by intragastric injection of 50 µg of tamoxifen (Sigma-Aldrich) per day for 3 consecutive days between P1 (P0 being the day of birth) and P5. For mice older than 6 weeks ("invalidation in adulthood", **Fig. 5, S7 and S8B**), recombination was induced by two gavages with 10 mg of tamoxifen each, at a 48 hours interval. Injection of LPS to induce the sickness response was performed at least 1 month and a half after tamoxifen treatment, to allow the full renewal of peripheral Cx3cr1$^{+}$ cells (Goldmann et al., 2013; Parkhurst et al., 2013; Peng et al., 2016; Wolf et al., 2013; Yona et al., 2013).

**Induction of Sickness behavior and body weight assessment**

Mice were injected intraperitoneally with 0.2 mg/kg LPS (O55:B5, Sigma-Aldrich L-6529) or control saline solution at 10:30 am. This dose of LPS induces a reliable expression of sickness behavior and >98% survival (data not shown). Body weight variation was used to assess sickness behavior, on male and female mice, separately, either "adult" (2-10 months old, matched between genotypes) or, in **Fig. 1C-D** and **Fig. S2C-D,** "aged" (12-18 months old, matched between genotypes). Mice were weighed daily at 10:30 am by an experimenter blind to the experimental conditions (treatment, genotype). Weight variation is expressed as percentage of the weight at the day of injection (Day 0). In some experiments, the weight was assessed over several days to study the time-course of recovery.

**Flow cytometry**

In the flow cytometry experiments, *Cx3cr1*$^{GFP/+}$*; Htr2b*$^{+/+}$ and *Cx3cr1*$^{GFP/+}$*; Htr2b*$^{-/-}$ adult mice, of both sexes, were used. As we observed no difference between males and females (data not shown), data obtained from both sexes were pooled. 24h after injection with LPS or saline solution, animals were anesthetized with pentobarbital, perfused with ice-cold PBS, and whole brain (cerebellum and olfactory bulbs removed) suspensions were prepared with a combination of enzymatic and mechanic treatments (NTDK kit, Miltenyi Biotec). The suspension was strained through a 70 µm nylon cell strainer, centrifuged, then cells were resuspended in 4 ml

30% isotonic Percoll (Sigma-Aldrich) and covered with 6 ml of PBS. After centrifugation, pelleted cells were washed extensively in PBS and resuspended in FACS buffer (PBS, 1% BSA, 1 mM EDTA). For the staining, Fc block was added 5 minutes prior to the relevant antibodies**,** either anti-CD45, -CD11b or -TREM2 (listed in **Table S1**). After incubation, cells were washed and DAPI (D1306, Invitrogen) was added to identify the dead cells. The gated population for the measurement of the Median Fluorescent Intensities (MFI) was: $DAPI^-$, singlet, $GFP^+$ ("$GFP^+$ population"). For CD45, we moreover distinguished $GFP^+CD45^{Lo}$ (microglia) from $GFP^+CD45^{Hi}$ (monocytes/macrophages) subpopulations. Flow cytometry analyses were performed on a VYB MacsQuant (Miltenyi Biotec).

**Quantification and morphological analysis of microglia:**

To allow microglia imaging and analysis in thick slices without immunostaining, like in (Verdonk et al., 2016), morphological analysis was performed on *Cx3cr1*$^{GFP/+}$*; Htr2b*$^{+/+}$ and *Cx3cr1*$^{GFP/+}$*; Htr2b*$^{-/-}$ mice. Two independent experiments have been performed, one on males and the other on females. All the samples within one experiment were processed simultaneously, but the male and the female experiments were not performed in the same time and therefore were analyzed separately. 24h after saline or LPS injection, mice were killed by lethal injection of pentobarbital (Vetoquinol, France), the brains were immediately removed, cut in a trans-sagittal plane in the inter-hemispheric fissure, and cerebral hemispheres were fixed during 24h in 4 % buffered paraformaldehyde (Sigma-Aldrich). Following fixation, tissue samples were sliced along a sagittal plane on a calibrated vibrating slicer (Microm 650V, ThermoScientific) into 100-µm-thick free-floating slices. Image acquisition and processing were performed as described in (Verdonk et al., 2016). Briefly, sample areas from the whole hippocampus of the most medial slice (one per animal) were acquired using a spinning disc confocal system (CellVoyager CV1000, Yokogawa, Japan) with a UPLSAPO 40×/NA 0.9 objective. Mosaic, volume creation and maximum projection processing from confocal images were done using ImageJ v1.50 software and analysis performed with AcapellaTM image analysis software (version 2.7, PerkinElmer Technologies, Waltham, USA). This allowed both to determine the microglial density and to analyse individual microglia. The average number of microglia reconstructed per animal was 200. For each microglia, different morphological criteria previously defined in (Verdonk et al., 2016) and illustrated in **Fig. 2E** were analyzed: its "number of segments", a segment being defined as the length of process between two nodes ; its "total ramification length", corresponding to the total length of its processes ; its "cell body area" ; and its "cell environment area" (named "covered environment area" in (Verdonk et al., 2016) which represents the total surface coverable by its ramifications and is calculated from the area of the polygon formed by linking the extremities of its processes, expressed in $\mu m^2$**.** Finally, the density of microglial cells was calculated by dividing the number of microglial cells by the scanned tissue area.

**Inflammatory cytokines and receptors array on primary microglia cultures.**

Primary microglia were prepared from pools of cortices from *Htr2b*$^{+/+}$or *Htr2b*$^{-/-}$ P0-P1 pups, not sex-typed (n=6 pups per culture), as previously described (Kolodziejczak et al., 2015; Roumier et al., 2008), and grown in DMEM (Invitrogen, France) with 10% heat-inactivated FCS (BioWest, France). Microglia were detached from the astrocytic layer between 12 and 14 days *in vitro* by gentle shaking and settled on 12-well plates. They were then activated with LPS (10 ng/ml) for 24 h.

Total RNA was isolated from primary microglia cultures using the RNeasy mini kit (Qiagen) and 500 ng of RNA from each culture were converted to cDNA using the $RT^2$ first strand kit (SABioscience, Qiagen). Quantitative mRNA expression was then measured using the inflammatory cytokines and receptors RT2 profiler PCR array (PAMM-011ZA, SABioscience, Qiagen), according to manufacturer's instructions on a Stratagene Mx3005P (Agilent) apparatus. The mRNA expression of each gene was normalized using the expression

of *Hsp90* and *Gapdh* as housekeeping genes and compared with the data obtained with the control group (*Htr2b*$^{+/+}$ microglia cultures treated with LPS) according to the $2^{-\Delta CT}$ method. Results are thus expressed as fold change from LPS-treated *Htr2b*$^{+/+}$ microglia cultures. Statistical analysis was performed using the Qiagen web resource.

**Quantitative real time PCR on brain tissue and data analysis**

These studies were performed on male mice. 4h or 24h after injection with LPS or 24h after saline injection, adult male mice were anesthetized with pentobarbital, perfused with ice-cold PBS, and the brains (cerebellum and olfactory bulbs removed) were extracted, frozen and kept at -80°C. Total RNAs was extracted using Trizol reagent (Invitrogen) and treated with DNase (Thermoscientific). First-strand cDNA was synthesized by reverse transcription of 2 µg of total RNA with Superscript-II reverse transcriptase (Invitrogen, Illkirch, France). Reverse transcriptase was omitted in samples as negative controls. Primers were designed with PrimerBlast (NCBI) (listed in **Table S2**). Relative expression levels of mRNAs were determined by real time RT-PCR using Absolute SYBR Green Mix (Thermoscientific) on a QuantStudio apparatus (Applied Biosystems). Efficiency of amplification for each primer pair was checked on a standard curve. Gene expression levels were normalized to mouse cyclophilin B mRNA expression using the $2^{-\Delta Ct}$ method.

Principal component analysis (PCA) and hierarchical clusterings were performed with R, using PCA and HCPC functions of the FactoMineR package (https://www.rdocumentation.org). Missing values (10% in total) were imputed with the MissMDA package. HCPC was performed on the first four dimensions of the PCA results, which represented 84-94% of the total inertia. Determination of the optimal number of clusters was based on the loss of inertia graph. Ellipses on PCA graphs represent the expected (95% confidence interval) locations of the barycenter of each condition.

**TaqMan assay on purified microglia.**

Microglia were isolated from pools of two or three P1 pups, not sex-typed**,** and from P8, P15, P30 and P60 individual male mice. Briefly, anesthetized mice were perfused with ice-cold PBS and the brains (cerebellum and olfactory bulbs removed) were enzymatically digested using the Neurodissociation kit (Miltenyi Biotec, Germany). To remove myelin and debris, cells were resuspended in 75% Percoll, overlayed with 25% Percoll and further with PBS. Samples were centrifuged at 800 g at 4°C for 45 min with no brake. The interphase containing mostly microglia was collected and incubated with anti-mouse CD11b magnetic beads (MACS Miltenyi) at 4°C for 15 min. CD11b positive populations were then isolated using MACS columns in a magnetic field and the purity (>90%) was controlled by flow cytometry. CD11b positive fraction was pelleted and lysed in lysis buffer from RNAaqueous-Microkit (Ambion). Lysates were frozen and stored at -80° C until total RNA extraction.

Total RNA was extracted using the RNAaqueous-Microkit (Ambion) and RNA was reverse-transcribed as described above. Amplification reaction was performed using the SsoAdvanced universal supermix (Biorad) and the PrimePCR probe assays for *Htr2b* **(**dMmuCPE5096701**),** *Hprt* (qMmuCID0005679) or *Nono* (qMmuCED0040697) in accordance to the manufacturer instructions on a QuantStudio apparatus (Applied Biosystems). As shown in **Fig. S1**, we checked that the expression of *Hprt* did not vary during development compared to *Nono*, indicating that both could be used as reference genes. Consistently, similar kinetics of *Htr2b* expression were observed with *Hprt* or *Nono* as reference genes. The results were processed according to the $2^{-\Delta Ct}$ method.

**Statistical analysis**

Means and SEM are represented in all graphs. The statistical tests, indicated in each figure, were performed with Prism7 (GraphPad software).

***Results***

**Lack of *Htr2b* exacerbates weight loss induced by a peripheral LPS injection.**

To assess if *Htr2b* deficiency impacted sickness response in mice, we injected $Htr2b^{+/+}$ and $Htr2b^{-/-}$ adult (3-10 months-old) male mice intraperitoneally with LPS or a saline solution, and weighted them 24h later. Weight loss after a peripheral immune challenge can be considered as an integrative parameter resulting from the combined effects of anorexia, anhedonia, decreased activity (and thus access to food and water) and metabolic changes. Being sensitive and followable over several days, it is useful to compare the intensity of sickness behavior in different conditions (J. Godbout et al., 2008; J. P. Godbout et al., 2005; Henry et al., 2008; Wohleb et al., 2012; Yirmiya, 1996)**.** Indeed, we observed a significantly larger LPS-induced weight loss in $Htr2b^{-/-}$ than in wild-type mice, 24h after the injection ($Htr2b^{+/+}$: - 3.7±0.4% *vs* $Htr2b^{-/-}$: - 5.9±0.6%, p=0.016) (**Fig. 1A).** Additional experiments showed no effect of genotype in the time-course of weight recovery (**Fig. 1B)**. As systemic inflammations are particularly detrimental in aged individuals, we analyzed whether the effect of *Htr2b* deficiency was maintained with ageing. In 12-18 months-old male mice, the lack of *Htr2b* similarly exacerbated the effects of LPS on body weight, 24h after the injection ($Htr2b^{+/+}$: - 6.1±0.9% *vs* $Htr2b^{-/-}$: - 9.7±1.5%, p=0.037) (**Fig. 1C**). Moreover, in aged males, the difference between $Htr2b^{-/-}$ and $Htr2b^{+/+}$ mice was protracted and still visible at D+2 (p=0.029 at D+1 and p=0.024 at D+2) (**Fig. 1D)**.

We repeated these experiments in females (**Fig. S2**). Although the effect of LPS on weight 24h after the injection seemed more pronounced in females than in males, a significant difference between genotypes was still observed, both in adult (**Fig. S2A**) and aged (**Fig. S2C**) females (adult: $Htr2b^{+/+}$: - 6.1±0.4% *vs* $Htr2b^{-/-}$: - 7.7±0.4%, p=0.039; aged $Htr2b^{+/+}$: - 7.0±0.6% *vs* $Htr2b^{-/-}$: - 9.6±1.0% p=0,033). We observed no effect of genotype on the time-course of recovery in females (**Fig. S2B and S2D**).

Altogether, these experiments demonstrate that the loss of *Htr2b* gene sensitizes animals to sickness response in adult males, as well as in females and in aged animals of either sex.

**Stronger reactivity of microglia to peripheral LPS injection in $Htr2b^{-/-}$ mice.**

Peripheral immune challenges can induce a central reaction and notably alterations in microglia inflammatory markers (Corona et al., 2010; Wohleb et al., 2012) and morphology (Kozlowski & Weimer, 2012), which may support the behavioral changes. We thus investigated, by flow cytometry and microscopy, whether the exacerbated weight loss in $Htr2b^{-/-}$ mice was associated to an increased microglial activation, 24h after treatment (**Fig. 2A**). For all these experiments, we used adult double transgenic mice in which microglia express GFP under the control of the *Cx3cr1* promoter (Jung et al., 2000): $Cx3cr1^{GFP/+}$*;* $Htr2b^{+/+}$ *vs* $Cx3cr1^{GFP/+}$*;* $Htr2b^{-/-}$.

As a first approach, we examined by flow cytometry the impact of LPS on the surface expression of several immune markers, in brain cell suspensions from adult $Cx3cr1^{GFP/+}$ mice either $Htr2b^{+/+}$ or $^{-/-}$ (note that for this analysis, data from males and females were pooled). We analyzed the expression of either CD45, CD11b or TREM2 in the $GFP^+$ (and singlet, $DAPI^-$) cell population (example in **Fig. 2B**). We observed that this $GFP^+$ population was composed on average by > 95% of microglial cells identified by their low to intermediate expression of CD45 ($GFP^+CD45^{Lo}$ cells), and by a small (< 4%) subset of $GFP^+CD45^{Hi}$ cells corresponding to monocytes/macrophages (example in **Fig. S3A**). These proportions were not affected by LPS injection, neither in $Htr2b^{+/+}$ nor $Htr2b^{-/-}$ mice (**Fig. S3B**), indicating that the treatment didn't induce a significant infiltration of monocytes/macrophages after 24h. Moreover, the small subset of monocytes/macrophages had little impact on the CD45 MFI in the whole $GFP^+$ population: indeed, the CD45 MFI in the $GFP^+$ population were strongly correlated to those among the pure microglia ($GFP^+CD45^{Lo}$) subpopulation (Pearson correlation coefficient = 0,99689), with an overestimation of +1,6% on average (**Fig S3C**). Based on this and on the low and stable percentage of monocytes/macrophages in the different conditions, we assumed that

in our experiments, MFI changes in the $GFP^+$ population would reflect those of microglia, even though the macrophage/monocyte subpopulation could also be affected. We observed that in the $GFP^+$ population, the LPS injection induced a significant upregulation of CD45 in both genotypes (**Fig. 2C**, p =0,021 for CD45 in *Htr2b*$^{+/+}$, and **Fig. 2D,** p=0,006 for CD45 in *Htr2b*$^{-/-}$), confirming a central immune reaction. In contrast to CD45, the MFI of CD11b and TREM2 were not modified by LPS in the control (*Htr2b*$^{+/+}$) genotype **(Fig. 2C**). However, they were both upregulated by LPS in the mutant (*Htr2b*$^{-/-}$) genotype **(Fig. 2D**, p=0,004 and p=0,039 for CD11b and TREM2, respectively). There was no significant difference for any of these markers between *Htr2b*$^{+/+}$ and *Htr2b*$^{-/-}$ mice in the saline condition (**Fig. S3D**). Altogether, the flow cytometry experiments thus show a stronger response of brain myeloid cells in *Htr2b*$^{-/-}$ mice than in controls after LPS injection, which is likely representative of a stronger microglial reaction.

As a second approach, we performed an in-depth analysis of hippocampal microglia morphology, 24h after the saline or LPS injection. The hippocampus is a region where microglial, neuronal and neurochemical changes have been reported in several models of peripheral inflammation (Albertini et al., 2018; Corona et al., 2010; D'Mello et al., 2013; Riazi et al., 2008; Wohleb et al., 2012). However, we knew that the treatment with a single moderate (0,2 mg/kg) dose of LPS may be insufficient to impact on microglia density or morphology in wild-type mice (Wendeln et al., 2018). Actually, significant changes in microglia shape at this time point and in this region are generally induced by doses 5 to 25 times higher (Buttini et al., 1996; Hoogland et al., 2015; Verdonk et al., 2016). Therefore, we didn't expect large changes in *Htr2b*$^{+/+}$ mice, but hypothesized that we may detect an overreaction in the *Htr2b*$^{-/-}$ mutants. We thus used an automated acquisition and reconstruction program to analyze the morphology of more than 800 microglia per experimental condition, as in (Verdonk et al., 2016), in addition to microglia density. Because of the reported sex-dependent variations in microglia morphology (Weinhard et al., 2018; Yanguas-Casás, 2020), we performed an experiment with males only **(Fig. 2F-G)**, and another one with females only **(Fig. S4)**. Several parameters, illustrated in **Fig. 2E,** were measured to describe each microglia: its number of ramification segments, its total ramification length, its cell body area**,** and its cell environment area, i.e. the surface delineated by the polygon linking the furthest extremities of its processes. In *Htr2b*$^{+/+}$ males, we observed that indeed, the morphological parameters we addressed were not significantly altered 24h after LPS injection (**Fig. 2F**, clear symbols). In contrast, in *Htr2b*$^{-/-}$ males, they were all significantly increased by LPS treatment (**Fig. 2F**, red symbols: number of segments per microglia p=0.013, total ramification length of microglia processes p=0.013**,** cell body area p=0.017, and cell environment area p=0.010). The density of microglia remained unchanged by LPS in either genotype (**Fig. 2G**). Repeating this experiment in females gave consistent results, although not identical, with a significant effect of LPS on *Htr2b*$^{-/-}$ but not *Htr2b*$^{+/+}$ animals for the number of segments per microglia (p=0.036), the total ramification length (p=0.021) and the cell body area (p=0.006), but not for the cell environment area (**Fig. S4A**). The microglia density in the females was, as in males, not significantly changed by LPS in either genotype (**Fig. S4B**).

Thus, the analysis of cell morphology confirms what the flow cytometry experiments suggested, i.e. that the loss of *Htr2b* gene results in a stronger reaction of microglia after LPS injection. To note is that even though there are some sex specificities in its expression, this overreaction is, like the enhanced weight loss, detectable both in males and in females.

**Stronger reactivity of *Htr2b*$^{-/-}$ primary microglial cultures to LPS.**

*Htr2b* gene is expressed in microglia (Kolodziejczak et al., 2015; Krabbe et al., 2012), and we have previously shown that, in culture, *Htr2b*$^{-/-}$ microglia overexpress some cytokine receptor genes (Kolodziejczak et al., 2015), indicating an activated phenotype. To determine whether *Htr2b*$^{-/-}$ microglia are intrinsically more responsive to LPS than *Htr2b*$^{+/+}$ microglia, we

performed a screen for inflammatory markers on primary microglia cultures prepared from pools of either *Htr2b*$^{+/+}$ or *Htr2b*$^{-/-}$ neonates (not sex-typed). Cultures were incubated with LPS for 24h and a quantitative mRNA expression analysis of 84 cytokines and receptors related to inflammation was conducted. 46 genes reached the detection threshold among which five, *Ccl6*, *Tnfrsf11b*, *Spp1*, *Csf1*, and *Ccl9*, showed significant increases in the LPS-treated *Htr2b*$^{-/-}$ versus *Htr2b*$^{+/+}$ microglia cultures (p=0.006, p=0.013, p=0.0004, p=0.017, p=0.030, respectively) (**Fig. 3A**). These data suggest that the absence of *Htr2b* skews microglia into a sensitive state characterized by an increased and particular response to LPS treatment.

**Prolonged neuroinflammation in *Htr2b*$^{-/-}$ mice after LPS treatment.**

We then analyzed these five markers by quantitative RT-PCR (qPCR), in the brain of *Htr2b*$^{+/+}$ and *Htr2b*$^{-/-}$ male mice, 4h and 24h after LPS or 24h after saline ("SAL") injection. We also assessed expression of Lipocalin-2 (*Lcn2*), Tnf-α (*Tnfa*), Interleukin-6 (*Il6*) and Interleukin-1ß (*Il1b*), which are known to be strongly induced by LPS (Cazareth et al., 2014; Golia et al., 2019; Ip et al., 2011; Kang et al., 2018) as well as *Hexb* and *Fcrls*, two genes specifically expressed in microglia (Hickman et al., 2013). In the saline condition, expression of these genes was similar in *Htr2b*$^{+/+}$ and *Htr2b*$^{-/-}$ brains. Four hours after LPS injection, expression of most of the tested genes had changed, but still with no significant difference between genotypes (**Fig. 3B)** except for *Il1b,* which was higher in *Htr2b*$^{-/-}$ brains (**Fig. S5**).

In contrast, 24h after LPS, a striking difference was noted between genotypes. In *Htr2b*$^{+/+}$ brains, most markers had returned to or remained similar to saline levels**,** consistent with previous studies reporting a rapid increase of expression of inflammatory cytokines in microglia, which returns almost back to normal after 12-24h (Norden et al., 2016). However, in *Htr2b*$^{-/-}$ brains, *Spp1*, *Ccl6* and *Lcn2* remained elevated in comparison with their saline group and were significantly overexpressed in comparison with the LPS-treated *Htr2b*$^{+/+}$ mice (p=0.0065, p<0.0001, p=0.0031, respectively) **(Fig. 3B)**; *Hexb* displayed a significant decreased expression in *Htr2b*$^{-/-}$ compared to *Htr2b*$^{+/+}$ brains (p=0.0323), and *Tnfrsf11b* decreased in wild-type but not in mutant mice. For *Ccl9, Csf1, Fcrls*, differences between genotypes were not significant **(Fig. 3B)**; *Tnfa* remained elevated and *Il6* and *Il1b* went back to basal level in both genotypes (**Fig S5**). In conclusion, these data showed that the exaggerated sickness behavior observed in *Htr2b*$^{-/-}$ mice is associated with a prolonged change in expression of a subset of inflammatory markers in brain (*Spp1, Ccl6, Lcn2, Tnfrsf11b, Hexb*).

To assess the overall picture of neuroinflammation variation, we applied a dimension reduction analysis to the qPCR data, by principle component analysis (PCA). As expected, we observed a clear separation between samples from the control ("SAL") and "LPS-4h" conditions. More interestingly, this analysis uncovered the position of "*Htr2b*$^{-/-}$ LPS-24h" samples as distinct from "saline" and "LPS-4h", whereas samples from wild-type mice 24h after LPS injection ("*Htr2b*$^{+/+}$ LPS-24h") were close to the "saline" samples **(Fig. 3C**). This difference between genotypes 24h after injection was confirmed by a hierarchical clustering analysis, which partitioned the samples into two main clusters **(Fig. 3D)**. Cluster 1 contained all the LPS-24h samples of the *Htr2b*$^{+/+}$ mice (quoted "WT" in the dendrogram) together with all the "saline" samples of both genotypes. In contrast, LPS-24h samples of *Htr2b*$^{-/-}$ mice (quoted "2B KO" in the dendrogram) were significantly enriched in cluster 2 (v test = 2,53, p=0.011), which contained all the LPS-4h samples of both genotypes. These multivariate analyses suggest that the absence of *Htr2b* mainly disrupts the resolution of the neuroinflammatory response, 24h after the immune challenge. Consistently with the flow cytometry and microglial morphology analyses, these results thus indicate a prolonged neuroinflammation in *Htr2b*$^{-/-}$ male mice in response to peripheral LPS injection.

As expression of the 5-$HT_{2B}$ receptor has been reported in some peripheral immune cells in humans (de Las Casas-Engel et al., 2013; Szabo et al., 2018), we investigated the impact of LPS treatment on the peripheral levels of Lcn2, Spp1 and Ccl6, whose gene expression was

prolonged in the brain of *Htr2b*$^{-/-}$ male mice after LPS (see above). The plasmatic levels of these cytokines were determined at 0, 4 and 24h after LPS injection in adult male mice (**Fig. S6**). LPS injection induced a strong increase after 4 or 24 hours depending on the cytokines. However, to the contrary of what we observed in the brain, we did not find significant differences in the plasma levels of these cytokines between *Htr2b*$^{+/+}$ and *Htr2b*$^{-/-}$ mice at any time-point. Together, these results suggest that the lack of 5-HT$_{2B}$ receptor does not modify the peripheral response for Lcn2, Spp1 and Ccl6 but specifically impacts on their brain expression 24h after LPS injection.

***Htr2b* expression in microglia changes during postnatal development.**

Our results above point to a role of microglia in the exacerbated response of *Htr2b*$^{-/-}$ mice to LPS, which would be consistent with the fact that these cells express *Htr2b* (Kolodziejczak et al., 2015; Krabbe et al., 2012). As the transcriptomic profile of microglia vary during development (Hammond et al., 2019; Matcovitch-Natan et al., 2016; Thion et al., 2018), we first examined *Htr2b* mRNA levels in microglia purified at different ages from P1 to P50-60. All animals were males except at P1, where each sample was a pool of pups, not sex-typed. As shown in **Fig. 4A**, we found that *Htr2b* expression in microglia is comparable at P1 and P8 and then is significantly increased at P15 ($p=0.030$) and P30 ($p=0.029$). We thus decided to test the impact of *Htr2b* invalidation in microglia either early (since birth) or in adulthood (invalidation after 6 weeks).

**A targeted and early deletion of *Htr2b* in microglia is sufficient to enhance the LPS-induced weight loss.**

The *Htr2b* gene expression has been described in microglia (Kolodziejczak et al., 2015; Krabbe et al., 2012), but also in serotonergic (Diaz et al., 2012) and dopaminergic (Doly et al., 2017) neurons, as well as in subsets of activated cells of the myeloid lineage in humans (de Las Casas-Engel et al., 2013; Szabo et al., 2018). To determine if the effect of *Htr2b* deletion on sickness behavior and neuroinflammation was specifically dependent on the microglial 5-HT$_{2B}$ receptors, we generated mice deleted for the *Htr2b* gene only in microglia. To this aim, *Cx3cr1*$^{CreERT2/+}$ mice (Parkhurst et al., 2013) were crossed with *Htr2b*$^{fl/fl}$ mice (Doly et al., 2017). We first investigated the effects of early loss of microglial *Htr2b* gene by treating newborn pups with tamoxifen, and injecting LPS or saline at 2-4 months of age (**Fig. 4B**). To check the deletion at the *Htr2b* locus in the brain, we sorted microglia and non-microglial cells and determined by qPCR that recombination at the *Htr2b* locus occurred specifically in microglia and not in other brain cells (**Fig. S7A-C**). To note is that in the periphery, it has been previously demonstrated that due to their high turn-over rate, peripheral CX3CR1$^{+}$ cells (monocytes, macrophages) that recombine at the time of tamoxifen injection are, at P30 at last, fully repopulated from their CX3CR1-negative bone marrow precursors (Goldmann et al., 2013; Parkhurst et al., 2013; Peng et al., 2016; Wolf et al., 2013; Yona et al., 2013). This is in contrast with microglia which are long-lived and self-renewing (Füger et al., 2017; Tay et al., 2017), and remain permanently recombined (Goldmann et al., 2013; Parkhurst et al., 2013; Peng et al., 2016; Wolf et al., 2013; Yona et al., 2013). Thus, this protocol results in adult mice bearing *Htr2b* recombination only in microglial cells.

We analyzed the sickness response in *Cx3cr1*$^{CreERT2/+}$*; Htr2b*$^{fl/fl}$ male mice and control littermates, all treated with tamoxifen at birth. We observed that weight loss 24h after LPS injection was significantly enhanced in the absence of microglial *Htr2b* (*Cx3cr1*$^{+/+}$*; Htr2b*$^{fl/fl}$: -4.5±0.3% *vs Cx3cr1*$^{CreERT2/+}$*; Htr2b*$^{fl/fl}$: - 6.8±0.6%; $p=0.0082$) (**Fig. 4C**), similar to the results in *Htr2b*$^{-/-}$ full knock-out mice (**Fig. 1A**). The effect was even more pronounced, as weight variations were still significantly different between *Cx3cr1*$^{CreERT2/+}$*; Htr2b*$^{fl/fl}$ mice and their littermates two days after LPS treatment ($p=0.004$ at D+2) (**Fig. 4D**). Thus, in males, when the *Htr2b* gene is deleted neonatally in microglia, the weight loss at 24h is significantly exacerbated and its recovery is delayed. When we replicated this experiment in females we observed a

consistent effect of *Htr2b* neonatal invalidation in microglia: *Cx3cr1*$^{CreERT2/+}$*; Htr2b*$^{fl/fl}$ female mice showed an exaggerated weight loss compared to their control littermates, with a significant difference at D+2 and D+3 (p=0.0076 and p=0.0048, respectively) (**Fig. S8A**).

**A targeted and early deletion of *Htr2b* in microglia is sufficient to sensitize to LPS-induced neuroinflammation.**

We next examined the effect of LPS injection on neuroinflammation in the brain of male *Cx3cr1*$^{CreERT2/+}$*; Htr2b*$^{fl/fl}$ and control mice. We focused on the time point in which differences of mRNA levels had been observed, i.e. 24h after treatment. Strikingly, we found, as previously in *Htr2b*$^{-/-}$ compared to *Htr2b*$^{+/+}$ mice, a significant overexpression of *Spp1* (p=0.030) and *Ccl6* (p=0.031) in *Cx3cr1*$^{CreERT2/+}$*; Htr2b*$^{fl/fl}$ brains compared to controls, in the LPS condition. mRNA levels of *Lcn2* and *Tnfrsf11b* were slightly although not significantly increased in *Cx3cr1*$^{CreERT2/+}$*; Htr2b*$^{fl/fl}$ mice (**Fig. 4E)**. Furthermore, mRNA levels of *Csf1* were also significantly higher in *Cx3cr1*$^{CreERT2/+}$*; Htr2b*$^{fl/fl}$ brains compared to controls (p=0.009) after LPS treatment, a difference that we hadn't observed between *Htr2b*$^{-/-}$ and *Htr2b*$^{+/+}$ mice. This suggests that the lack of 5-$HT_{2B}$ receptor in cells other than microglia, probably serotonergic or dopaminergic neurons based on *Htr2b* expression profile (Diaz et al., 2012; Doly et al., 2017), may inhibit the increased *Csf1* expression upon LPS injection, this increased expression being revealed when the *Htr2b* is invalidated in microglia only. In control condition (saline injection), no significant difference was found between genotypes.

A PCA representation showed that "LPS 24h" samples from male mice invalidated for microglial *Htr2b* since birth (quoted "*Cx3cr1*$^{creER/+}$ + TX-Birth LPS 24h") were far from all the others (**Fig. 4F)**. Consistently, a hierarchical clustering analysis partitioned the samples in two groups: cluster 1 which contained all the saline-treated mice and the majority of LPS-treated mice of the control genotype (quoted "Cx3 +/+ LPS 24h" in the dendrogram); and cluster 2 which was characterized by its enrichment in LPS-treated mutant ("Cx3 creER/+ LPS 24h" in the dendrogram) mice (v test = 3,69), p=0.0002) (**Fig. 4G)**.

Altogether, these data show that early deletion of microglial *Htr2b* results in an enhanced LPS-induced weight loss associated, in males**,** with an increased expression of neuroinflammation-associated genes at 24h post-LPS injection.

**Deletion of microglial *Htr2b* in adulthood does not sensitize to LPS-induced weight loss nor to LPS-induced neuroinflammation.**

To determine whether expression of microglial 5-$HT_{2B}$ receptor is also important later at the time of the sickness episode, we induced *Htr2b* recombination in adulthood. To this aim, adult *Cx3cr1*$^{CreERT2/+}$*; Htr2b*$^{fl/fl}$ male mice (>6 weeks) underwent tamoxifen gavage. We checked that this protocol was as efficient as neonatal treatment to induce gene recombination (**Fig. S7C**). Mice were injected with LPS or saline solution at least one month and a half after the tamoxifen treatment (**Fig. 5A**), to allow renewal of peripheral myeloid cells (Parkhurst et al., 2013). In this condition, *Cx3cr1*$^{CreERT2/+}$*; Htr2b*$^{fl/fl}$ male mice exhibited the same weight variation and kinetics of recovery upon LPS injection as their control littermates (**Fig. 5B-C**), in contrast to the enhanced weight loss observed when microglial *Htr2b* had been removed neonatally (**Fig. 4A-C**). Thus, late ablation of the microglial *Htr2b* does not impact on the weight loss induced by LPS injection in males. Replicating this experiment in females led to the same observation: no difference in weight loss upon LPS could be detected between *Cx3cr1*$^{CreERT2/+}$*; Htr2b*$^{fl/fl}$ females and their littermates if the tamoxifen treatment had taken place in adulthood (**Fig. S8B**).

We next analyzed the expression of the same inflammatory markers as previously, in the brain of *Cx3cr1*$^{CreERT2/+}$*; Htr2b*$^{fl/fl}$ and control adult male mice, 24h after LPS injection. In contrast to the enhanced expression of several inflammatory markers, observed when microglial *Htr2b* was deleted at birth, we did not find any significant difference of mRNA expression levels for any of the tested markers between *Cx3cr1*$^{CreERT2/+}$*; Htr2b*$^{fl/fl}$ and their control littermates treated with tamoxifen in adulthood (**Fig. 5D**). Consistantly, neither PCA nor

hierarchical clustering could discriminate the samples of mice invalidated for *Htr2b* in adulthood from their control littermates. The main difference among samples was due to the treatment (saline *vs.* LPS) (**Fig. 5E-F**). Thus, in contrast with full or microglial neonatal invalidation, invalidation of the *Htr2b* gene in microglia at the adult stage does not change the time-course of neuroinflammation, for the genes we analyzed, which is consistent with the unchanged weight loss and recovery.

## *Discussion*

This study was designed to test the role of the 5-$HT_{2B}$ receptor gene, which is expressed notably in microglia, in the response to a peripheral immune challenge. We showed that the absence of *Htr2b*, the 5-$HT_{2B}$ receptor gene, is associated to enhanced weight loss, increased microglial activation and prolonged neuroinflammation after a peripheral LPS injection. The use of conditional knock-out mice allowed us to precisely point out that the lack of *Htr2b* specifically in microglia in the neonatal period, and not during adulthood, is responsible for these effects. Our results thus identify *Htr2b* as a new gene controlling sickness behavior, and highlight the role of microglia in gating the intensity and duration of the response to a peripheral immune challenge. In addition, our data suggest that a developmental instruction of microglia through 5-$HT_{2B}$ receptor is required during the neonatal period to limit the responsiveness to inflammatory stimuli in adulthood.

**Lack of *Htr2b* exacerbates the severity of sickness response and prolongs neuroinflammation**

Previous studies identified, among others, the membrane receptors CX3CR1 (Corona et al., 2010), IL-1R (Zhu et al., 2010), and the dimerization of glucocorticoid receptors (Silverman et al., 2013), as crucial to limit various aspects of the response to a peripheral inflammation. The first part of our study, based on full *Htr2b*$^{-/-}$ mice, identifies the serotonin receptor 5-$HT_{2B}$ as another regulator, whose impaired expression significantly changes short and long-term impacts of peripheral inflammations. Here, precisely, we discover a role of *Htr2b* in the control of the weight loss (both in adult and aged, males and females, mice), and of the time-course of the neuroinflammation (which we investigated in adult males), induced by a peripheral injection of LPS. Indeed, after a first phase (t = 4h), where the neuroinflammatory response was similar in wild-type and *Htr2b*$^{-/-}$ mice (except for *Il1b*), the expression of several inflammatory markers remained abnormally high (*Spp1, Ccl6*, *Lcn2*, *Tnfrsf11b*) or, to the contrary, were down-regulated to a larger extent (*Hexb*), in *Htr2b*$^{-/-}$ mice vs. wild-type, 24h after the immune challenge. This is illustrated by the segregation of the "*Htr2b*$^{-/-}$ LPS 24h" samples in the principal component analysis and the hierarchical clustering.

**Invalidation of *Htr2b* in microglia only, since birth, recapitulates the phenotype of enhanced weight loss and prolonged neuroinflammation**

As *Htr2b* is expressed in microglia (Kolodziejczak et al., 2015; Krabbe et al., 2012), serotonergic (Diaz et al., 2012) and dopaminergic neurons (Doly et al., 2017), and, at least in Humans, in subsets of cells of the myeloid lineage (de Las Casas-Engel et al., 2013; Szabo et al., 2018), we used the tamoxifen-inducible *Cx3cr1*$^{CreERT2}$ line (Parkhurst et al., 2013) to specifically assess the contribution of the microglial *Htr2b*. Besides leaving the other (i.e. Cx3cr1-negative) cell types untouched, this procedure is a validated strategy to obtain mice with recombined microglia, but normal peripheral monocytes and macrophages cells. Indeed, although peripheral Cx3cr1-positive cells recombine, like microglial cells, after the tamoxifen treatment, they are immediately and progressively renewed from Cx3cr1-negative precursors, and after one month, 95-99% of the peripheral myeloid cells are normal, non-recombined (Goldmann et al., 2013; Parkhurst et al., 2013; Peng et al., 2016; Wolf et al., 2013; Yona et al., 2013).

Here, *Cx3cr1*$^{CreERT2/+}$*; Htr2b*$^{fl/fl}$ neonates were treated with tamoxifen between P0 and P5 to induce *Htr2b* recombination neonatally, and submitted to the peripheral immune challenge at least two months later. This selective invalidation was sufficient to phenocopy the alterations observed in full *Htr2b*$^{-/-}$ male mice: enhanced severity of LPS-induced weight loss and of neuroinflammation, which thus points to a role of microglia in the phenotype. Nevertheless, to note is that formally, a complementary contribution from the transiently *Htr2b*-recombinated peripheral Cx3cr1-positive cells, before their replacement by non recombined cells, can not be excluded. This would imply that these peripheral mutated cells interfere, during their short existence, with brain development, through a yet-to-be-defined mechanism, and that it modifies the later responsiveness to LPS. This possibility is highly speculative in the current state of knowledge, but it may add to the, likely, main contribution of microglia to the phenotype.

**Developmental role of the microglial 5-HT$_{2B}$ receptor in controlling the response to a peripheral immune challenge: putative mechanisms**

Tamoxifen-induced invalidation of *Htr2b* at birth in the *Cx3cr1*$^{CreERT2/+}$*; Htr2b*$^{fl/fl}$ mice sensitizes to the response to a peripheral LPS injection, most likely by modifying primarily microglia (see above). Importantly, in contrast, the induction of microglial *Htr2b* invalidation in adulthood (i.e. at 6 weeks of age) does not modify the course of the neuroinflammatory nor the behavioral response to a subsequent LPS injection. To note is that, on a methodological level, the absence of phenotype in *Cx3cr1*$^{CreERT2/+}$*; Htr2b*$^{fl/fl}$ mice treated with tamoxifen in adulthood clearly indicates that the exacerbated effects seen in the animals of this same genotype, but treated with tamoxifen at birth, are due to the absence of *Htr2b* and not to their heterozygosity for *Cx3cr1*. Comparison of the effects of *Htr2b* invalidation at these two time-points also identifies a developmental critical period, included between birth and 6 weeks of age, for the microglial 5-HT$_{2B}$ receptor: if it is not expressed during this time-window, animals will later overreact to inflammatory stimuli.

How can a neonatal, and not an adult, alteration of microglia have this protracted effect on sickness behavior and neuroinflammation? We propose two non-exclusive interpretations. The first one is that microglia, in the absence of 5-HT$_{2B}$ receptor, do not mature properly and remain or become hyperreactive. This “microglia-autonomous” hypothesis is supported by the increased levels of inflammatory markers in *Htr2b* $^{-/-}$, vs *Htr2b*$^{+/+}$, primary cultures of microglia, observed here after LPS treatment, and previously in basal condition (Kolodziejczak et al., 2015). The effects of LPS injection on microglia revealed by flow cytometry and morphology analysis, and specific to *Htr2b*$^{-/-}$, not control, mice, are also consistent with an intrinsic microglial maturation defect. As the late (24h) neuroinflammation is particularly enhanced in the absence of microglial *Htr2b*, the mutated microglia may be defective in getting back to a basal activation state. By promoting a prolonged neuroinflammation, this would maintain in a state of altered neuronal activity the brain regions controlling for example the motivation for food and thus the weight loss. The second interpretation for the effect of the neonatal, but not adult, microglia *Htr2b* invalidation, is that the early lack of 5-HT$_{2B}$ receptor impacts on microglial functions particularly important for brain development. Indeed, the neonatal period that we identified as crucial for the expression of *Htr2b* in microglia spans over important steps of neurodevelopment. Microglia contribute actively to synaptogenesis, brain wiring, and synaptic refinement (Thion & Garel, 2017). Moreover, we know that serotonin triggers an oriented growth of microglial processes (Kolodziejczak et al., 2015). This may regulate the interaction of microglia with surroundings neurons. Thus, in place or in addition to intrinsic changes in microglia, the lack of microglial *Htr2b* in the neonatal period may impact on brain development, making it more prone to induce sickness behavior and less efficient in controlling neuroinflammation in adulthood.

**A possible role of serotonin in microglia development and function**

Our study uncovered a role for the microglial 5-$HT_{2B}$ receptor, and an increase of its expression, during the neonatal period. This raises the question of how the receptor is activated during this critical time-window. Noteworthy, serotonergic axons are already present in all brain regions at birth, and their density increases in the first two to four postnatal weeks (Lidov & Molliver, 1982; Maddaloni et al., 2017). The high density of serotonergic axons, associated to the micrometer range of action of serotonin (Bunin & Wightman, 1998; Descarries et al., 1990) and the expression of 5-$HT_{2B}$ receptor in microglia, make thus feasible for serotonin to instruct the developing microglia over the whole brain during the neonatal period. Serotonin is known as a developmental factor for several brain structures, and modifying its level early induces long term effects on brain wiring and behavior (Gaspar et al., 2003; Shah et al., 2018; Teissier et al., 2017). Neonatal exposure to selective serotonin reuptake inhibitors (SSRI), which increases serotonin level, favors anxiety in adulthood (Ansorge et al., 2004; Teissier et al., 2015), while early tryptophan depletion decreases social interactions (Rok-Bujko et al., 2012; Zhang et al., 2006; Zoratto et al., 2013). Our results suggest that such early changes in serotonin levels may also impact on microglia and on the response to a subsequent peripheral inflammation. It would thus be interesting, in the future, to test if early exposure to SSRI or tryptophan depletion alters microglia through transcriptomic or epigenetic effects, a mode of regulation recently implicated in the control of microglia reactivity (Wendeln et al., 2018), and on the response to a peripheral immune challenge in adulthood.

**Significance and perspectives**

This study showed that in males, lack of microglial *Htr2b* during the neonatal period enhances the weight loss and prolongs the neuroinflammation induced by a peripheral immune challenge at adult stage. As the weight loss is also enhanced in females (full and conditional knock-outs), and in aged animals (at least in full knock-outs, both males and females), it would be interesting in a follow-up study to address if the same neuroinflammatory markers are prolonged in all conditions or whether there are sex- or age-dependent specificities.

Here, we uncovered a role for the microglial 5-$HT_{2B}$ receptor during the neonatal period. We nevertheless observed that the gene remains expressed in adulthood. Microglia exert various functions along a lifetime and there are other examples of microglial genes, which deletion has different impacts depending of the stage when it is induced, like *Dicer* or the histone deacetylases *Hdac1* and *Hdac2* (Datta et al., 2018; Varol et al., 2017). Further experiments will thus be required to determine the role of 5-$HT_{2B}$ receptor in adult microglia.

Finally, neuroinflammation is prominent in neurodegenerative and some psychiatric diseases. Our results therefore open perspectives on whether controlling microglia through 5-$HT_{2B}$ receptor could have a beneficial impact in some mental disorders or neurodegenerative diseases.

***References***


Albertini, G., Deneyer, L., Ottestad-Hansen, S., Zhou, Y., Ates, G., Walrave, L., Demuyser, T., Bentea, E., Sato, H., De Bundel, D., Danbolt, N. C., Massie, A., & Smolders, I. (2018). Genetic deletion of xCT attenuates peripheral and central inflammation and mitigates LPS-induced sickness and depressive-like behavior in mice. *Glia, 43*(20), 98.

Ansorge, M. S., Zhou, M., Lira, A., Hen, R., & Gingrich, J. A. (2004). Early-life blockade of the 5-HT transporter alters emotional behavior in adult mice. *Science, 306*(5697), 879-881.

Baganz, N. L., & Blakely, R. D. (2013). A dialogue between the immune system and brain, spoken in the language of serotonin. *ACS Chem Neurosci, 4*(1), 48-63.

Belmer, A., Quentin, E., Diaz, S. L., Guiard, B. P., Fernandez, S. P., Doly, S., Banas, S. M., Pitychoutis, P. M., Moutkine, I., Muzerelle, A., Tchenio, A., Roumier, A., Mameli, M., & Maroteaux, L. (2018). Positive regulation of raphe serotonin neurons by serotonin 2B receptors. *Neuropsychopharmacolgy, 43*, 1623–1632.

Bevilacqua, L., Doly, S., Kaprio, J., Yuan, Q., Tikkanen, R., Paunio, T., Zhou, Z., Wedenoja, J., Maroteaux, L., Diaz, S., Belmer, A., Hodgkinson, C., Dell'Osso, L., Suvisaari, J., Coccaro, E., Rose, R., Peltonen, L., Virkkunen, M., & Goldman, D. (2010). A population-specific HTR2B stop codon predisposes to severe impulsivity. *Nature, 468*(8), 1061-1066.

Bunin, M. A., & Wightman, R. M. (1998). Quantitative Evaluation of 5-Hydroxytryptamine (Serotonin) Neuronal Release and Uptake: An Investigation of Extrasynaptic Transmission. *J Neurosci, 18*(13), 4854-4860.

Buttini, M., Limonta, S., & Boddeke, H. W. (1996). Peripheral administration of lipopolysaccharide induces activation of microglial cells in rat brain. *Neurochemistry International, 29*(1), 25-35.

Cazareth, J., Guyon, A., Heurteaux, C., Chabry, J., & Petit-Paitel, A. (2014). Molecular and cellular neuroinflammatory status of mouse brain after systemic lipopolysaccharide challenge: importance of CCR2/CCL2 signaling. *J Neuroinflamm, 11*, 132.

Corona, A. W., Huang, Y., O'Connor, J. C., Dantzer, R., Kelley, K. W., Popovich, P. G., & Godbout, J. P. (2010). Fractalkine receptor (CX3CR1) deficiency sensitizes mice to the behavioral changes induced by lipopolysaccharide. *J Neuroinflamm, 7*, 93.

Cunningham, C. (2013). Microglia and neurodegeneration: the role of systemic inflammation. *Glia, 61*(1), 71-90.

D'Mello, C., Riazi, K., Le, T., Stevens, K. M., Wang, A., McKay, D. M., Pittman, Q. J., & Swain, M. G. (2013). P-selectin-mediated monocyte-cerebral endothelium adhesive interactions link peripheral organ inflammation to sickness behaviors. *J Neurosci, 33*(37), 14878-14888.

Dantzer, R., O'Connor, J. C., Freund, G. G., Johnson, R. W., & Kelley, K. W. (2008). From inflammation to sickness and depression: when the immune system subjugates the brain. *Nat Rev Neurosci, 9*(1), 46-56.

Datta, M., Staszewski, O., Raschi, E., Frosch, M., Hagemeyer, N., Tay, T. L., Blank, T., Kreutzfeldt, M., Merkler, D., Ziegler-Waldkirch, S., Matthias, P., Meyer-Luehmann, M., & Prinz, M. (2018). Histone Deacetylases 1 and 2 Regulate Microglia Function during Development, Homeostasis, and Neurodegeneration in a Context-Dependent Manner. *Immunity, 48*(3), 514-529.e516.

de Las Casas-Engel, M., Domínguez-Soto, A., Sierra-Filardi, E., Bragado, R., Nieto, C., Puig-Kroger, A., Samaniego, R., Loza, M., Corcuera, M. T., Gómez-Aguado, F., Bustos, M., Sánchez-Mateos, P., & Corbí, A. L. (2013). Serotonin skews human macrophage polarization through HTR2B and HTR7. *J Immunol, 190*(5), 2301-2310.

Descarries, L., Audet, M. A., Doucet, G., Garcia, S., Oleskevich, S., Séguéla, P., Soghomonian, J. J., & Watkins, K. C. (1990). Morphology of central serotonin neurons. Brief review of

quantified aspects of their distribution and ultrastructural relationships. *Ann N Y Acad Sci, 600*, 81-92.

Diaz, S. L., Doly, S., Narboux-Nême, N., Fernandez, S., Mazot, P., Banas, S., Boutourlinsky, K., Moutkine, I., Belmer, A., Roumier, A., & Maroteaux, L. (2012). 5-HT2B receptors are required for serotonin-selective antidepressant actions. *Mol Psychiatry, 17*, 154-163.

Doly, S., Quentin, E., Eddine, R., Tolu, S., Fernandez, S., Bertran-Gonzalez, J., Valjent, E., Belmer, A., Viñals, X., Callebert, J., Faure, P., Meye, F., Hervé, D., Robledo, P., Mameli, M., Launay, J., Maldonado, R., & Maroteaux, L. (2017). Serotonin 2B receptors in mesoaccumbens dopamine pathway regulate cocaine responses. *J Neurosci, 37*(43), 10372-10388.

El Oussini, H., Bayer, H., Scekic-Zahirovic, J., Vercruysse, P., Sinniger, J., Dirrig-Grosch, S., Dieterlé, S., Echaniz-Laguna, A., Larmet, Y., Müller, K., Weishaupt, J. H., Thal, D. R., van Rheenen, W., van Eijk, K., Lawson, R., Monassier, L., Maroteaux, L., Roumier, A., Wong, P. C., van den Berg, L. H., Ludolph, A. C., Veldink, J. H., Witting, A., & Dupuis, L. (2016). Serotonin 2B receptor slows disease progression and prevents degeneration of spinal cord mononuclear phagocytes in amyotrophic lateral sclerosis. *Acta Neuropathol, 131*(3), 465-480.

Füger, P., Hefendehl, J. K., Veeraraghavalu, K., Wendeln, A.-C., Schlosser, C., Obermüller, U., Wegenast-Braun, B. M., Neher, J. J., Martus, P., Kohsaka, S., Thunemann, M., Feil, R., Sisodia, S. S., Skodras, A., & Jucker, M. (2017). Microglia turnover with aging and in an Alzheimer's model via long-term in vivo single-cell imaging. *Nature Neuroscience, 20*(10), 1371-1376.

Gaspar, P., Cases, O., & Maroteaux, L. (2003). The developmental role of serotonin: news from mouse molecular genetics. *Nat Rev Neurosci, 4*(12), 1002-1012.

Godbout, J., Moreau, M., Lestage, J., Chen, J., Sparkman, N., O'Connor, J., Castanon, N., Kelley, K., Dantzer, R., & Johnson, R. (2008). Aging exacerbates depressive-like behavior in mice in response to activation of the peripheral innate immune system. *Neuropsychopharmacolgy, 33*(10), 2341-2351.

Godbout, J. P., Chen, J., Abraham, J., Richwine, A. F., Berg, B. M., Kelley, K. W., & Johnson, R. W. (2005). Exaggerated neuroinflammation and sickness behavior in aged mice following activation of the peripheral innate immune system. *FASEB J, 19*(10), 1329-1331.

Goldmann, T., Wieghofer, P., Müller, P. F., Wolf, Y., Varol, D., Yona, S., Brendecke, S. M., Kierdorf, K., Staszewski, O., Datta, M., Luedde, T., Heikenwalder, M., Jung, S., & Prinz, M. (2013). A new type of microglia gene targeting shows TAK1 to be pivotal in CNS autoimmune inflammation. *Nature Neuroscience, 16*(11), 1618-1626.

Golia, M. T., Poggini, S., Alboni, S., Garofalo, S., Ciano Albanese, N., Viglione, A., Ajmone-Cat, M. A., St-Pierre, A., Brunello, N., Limatola, C., Branchi, I., & Maggi, L. (2019). Interplay between inflammation and neural plasticity: Both immune activation and suppression impair LTP and BDNF expression. *Brain, Behavior, and Immunity, 81*, 484-494.

Hammond, T. R., Dufort, C., Dissing-Olesen, L., Giera, S., Young, A., Wysoker, A., Walker, A. J., Gergits, F., Segel, M., Nemesh, J., Marsh, S. E., Saunders, A., Macosko, E., Ginhoux, F., Chen, J., Franklin, R. J. M., Piao, X., Mccarroll, S. A., & Stevens, B. (2019). Single-Cell RNA Sequencing of Microglia throughout the Mouse Lifespan and in the Injured Brain Reveals Complex Cell-State Changes. *Immunity, 50*(1), 253-271.e256.

Henry, C. J., Huang, Y., Wynne, A., Hanke, M., Himler, J., Bailey, M. T., Sheridan, J. F., & Godbout, J. P. (2008). Minocycline attenuates lipopolysaccharide (LPS)-induced neuroinflammation, sickness behavior, and anhedonia. *J Neuroinflamm, 5*, 15.

Hickman, S. E., Kingery, N. D., Ohsumi, T. K., Borowsky, M. L., Wang, L.-c., Means, T. K., & El Khoury, J. (2013). The microglial sensome revealed by direct RNA sequencing. *Nature Neuroscience, 16*(12), 1896-1905.

Hoogland, I. C. M., Houbolt, C., van Westerloo, D. J., van Gool, W. A., & van de Beek, D. (2015). Systemic inflammation and microglial activation: systematic review of animal experiments. *J Neuroinflamm, 12*, 114.

Ip, J. P. K., Noçon, A. L., Hofer, M. J., Lim, S. L., Müller, M., & Campbell, I. L. (2011). Lipocalin 2 in the central nervous system host response to systemic lipopolysaccharide administration. *J Neuroinflam, 8*(1), 124.

Jung, S., Aliberti, J., Graemmel, P., Sunshine, M. J., Kreutzberg, G. W., Sher, A., & Littman, D. R. (2000). Analysis of fractalkine receptor CX(3)CR1 function by targeted deletion and green fluorescent protein reporter gene insertion. *Mol Cell Biol, 20*(11), 4106-4114.

Kang, S. S., Ren, Y., Liu, C.-C., Kurti, A., Baker, K. E., Bu, G., Asmann, Y., & Fryer, J. D. (2018). Lipocalin-2 protects the brain during inflammatory conditions. *Mol Psychiatry, 23*(2), 344-350.

Kolodziejczak, M., Bechade, C., Gervasi, N., Irinopoulou, T., Banas, S. M., Cordier, C., Rebsam, A., Roumier, A., & Maroteaux, L. (2015). Serotonin modulates developmental microglia via 5-HT2B receptors: potential implication during synaptic refinement of retinogeniculate projections. *ACS Chem Neurosci, 6*(7), 1219-1230.

Kozlowski, C., & Weimer, R. M. (2012). An automated method to quantify microglia morphology and application to monitor activation state longitudinally in vivo. *PLoS ONE, 7*(2), e31814.

Krabbe, G., Matyash, V., Pannasch, U., Mamer, L., Boddeke, H. W. G. M., & Kettenmann, H. (2012). Activation of serotonin receptors promotes microglial injury-induced motility but attenuates phagocytic activity. *Brain Behav Immun, 26*(3), 419-428.

Lidov, H. G., & Molliver, M. E. (1982). Immunohistochemical study of the development of serotonergic neurons in the rat CNS. *Brain Res Bulletin, 9*(1-6), 559-604.

Maddaloni, G., Bertero, A., Pratelli, M., Barsotti, N., Boonstra, A., Giorgi, A., Migliarini, S., & Pasqualetti, M. (2017). Development of Serotonergic Fibers in the Post-Natal Mouse Brain. *Front Cell Neurosci, 11*, 202.

Matcovitch-Natan, O., Winter, D. R., Giladi, A., Vargas Aguilar, S., Spinrad, A., Sarrazin, S., Ben-Yehuda, H., David, E., Zelada González, F., Perrin, P., Keren-Shaul, H., Gury, M., Lara-Astaiso, D., Thaiss, C. A., Cohen, M., Bahar Halpern, K., Baruch, K., Deczkowska, A., Lorenzo-Vivas, E., Itzkovitz, S., Elinav, E., Sieweke, M. H., Schwartz, M., & Amit, I. (2016). Microglia development follows a stepwise program to regulate brain homeostasis. *Science, 353*(6301), aad8670.

Montalvo-Ortiz, J. L., Zhou, H., D'Andrea, I., Maroteaux, L., Lori, A., Smith, A., Ressler, K., Nuñez, Y. Z., Farrer, L. A., Zhao, H., Kranzler, H. R., & J., G. (2018). Translational studies support a role for serotonin 2B receptors in aggression-related cannabis response. *Mol Psychiatry, 23*(12), 2277-2286.

Nebigil, C. G., Choi, D.-S., Dierich, A., Hickel, P., Le Meur, M., Messaddeq, N., Launay, J.-M., & Maroteaux, L. (2000). Serotonin 2B receptor is required for heart development. *Proc Natl Acad Sci U S A, 97*, 9508-9513.

Norden, D. M., Trojanowski, P. J., Villanueva, E., Navarro, E., & Godbout, J. P. (2016). Sequential activation of microglia and astrocyte cytokine expression precedes increased Iba-1 or GFAP immunoreactivity following systemic immune challenge. *Glia, 64*(2), 300-316.

Parkhurst, C N., Yang, G., Ninan, I., Savas, J N., Iii, J R. Y., Lafaille, J J., Hempstead, B L., Littman, D R., & Gan, W.-B. (2013). Microglia Promote Learning-Dependent Synapse Formation through Brain-Derived Neurotrophic Factor. *Cell, 155*(7), 1596-1609.

Peng, J., Gu, N., Zhou, L., B Eyo, U., Murugan, M., Gan, W.-B., & Wu, L.-J. (2016). Microglia and monocytes synergistically promote the transition from acute to chronic pain after nerve injury. *Nature Communications, 7*, 12029.

Perry, V. H., & Holmes, C. (2014). Microglial priming in neurodegenerative disease. *Nature Rev Neurol, 10*(4), 217-224.

Pitychoutis, P., Belmer, A., Moutkine, I., Adrien, J., & Maroteaux, L. (2015). Mice lacking the serotonin Htr2B receptor gene present an antipsychotic-sensitive schizophrenic-like phenotype. *Neuropsychopharmacolgy, 40*(12), 2764-2773.

Riazi, K., Galic, M. A., Kuzmiski, J. B., Ho, W., Sharkey, K. A., & Pittman, Q. J. (2008). Microglial activation and TNFalpha production mediate altered CNS excitability following peripheral inflammation. *Proc Natl Acad Sci U S A, 105*(44), 17151-17156.

Rivest, S. (2009). Regulation of innate immune responses in the brain. *Nat Rev Immunol, 9*(6), 429-439.

Rok-Bujko, P., Krząścik, P., Szyndler, J., Kostowski, W., & Stefański, R. (2012). The influence of neonatal serotonin depletion on emotional and exploratory behaviours in rats. *Behav Br Res, 226*(1), 87-95.

Roumier, A., Pascual, O., Bechade, C., Wakselman, S., Poncer, J. C., Real, E., Triller, A., & Bessis, A. (2008). Prenatal activation of microglia induces delayed impairment of glutamatergic synaptic function. *PLoS ONE, 3*(7), e2595.

Shah, R., Courtiol, E., Castellanos, F. X., & Teixeira, C. M. (2018). Abnormal Serotonin Levels During Perinatal Development Lead to Behavioral Deficits in Adulthood. *Front Behav Neurosci, 12*, 114.

Silverman, M. N., Mukhopadhyay, P., Belyavskaya, E., Tonelli, L. H., Revenis, B. D., Doran, J. H., Ballard, B. E., Tam, J., Pacher, P., & Sternberg, E. M. (2013). Glucocorticoid receptor dimerization is required for proper recovery of LPS-induced inflammation, sickness behavior and metabolism in mice. *Mol Psychiatry, 18*(9), 1006-1017.

Szabo, A., Gogolak, P., Koncz, G., Foldvari, Z., Pazmandi, K., Miltner, N., Poliska, S., Bacsi, A., Djurovic, S., & Rajnavolgyi, E. (2018). Immunomodulatory capacity of the serotonin receptor 5-HT2B in a subset of human dendritic cells. *Scientific reports, 8*(1), 1765.

Tay, T. L., Béchade, C., D'Andrea, I., St-Pierre, M.-K., Henry, M. S., Roumier, A., & Tremblay, M.-E. (2018). Microglia Gone Rogue: Impacts on Psychiatric Disorders across the Lifespan. *Front Mol Neurosci, 10*, 421.

Tay, T. L., Mai, D., Dautzenberg, J., Fernández-Klett, F., Lin, G., Sagar, Datta, M., Drougard, A., Stempfl, T., Ardura-Fabregat, A., Staszewski, O., Margineanu, A., Sporbert, A., Steinmetz, L. M., Pospisilik, J. A., Jung, S., Priller, J., Grün, D., Ronneberger, O., & Prinz, M. (2017). A new fate mapping system reveals context-dependent random or clonal expansion of microglia. *Nature Neuroscience, 20*(6), 793-803.

Teissier, A., Chemiakine, A., Inbar, B., Bagchi, S., Ray, R. S., Palmiter, R. D., Dymecki, S. M., Moore, H., & Ansorge, M. S. (2015). Activity of Raphé Serotonergic Neurons Controls Emotional Behaviors. *Cell reports, 13*(9), 1965-1976.

Teissier, A., Soiza-Reilly, M., & Gaspar, P. (2017). Refining the Role of 5-HT in Postnatal Development of Brain Circuits. *Front Cell Neurosci, 11*, 139.

Thion, M. S., & Garel, S. (2017). On place and time: microglia in embryonic and perinatal brain development. *Curr Opin Neurobiol, 47*, 121-130.

Thion, M. S., Low, D., Silvin, A., Chen, J., Grisel, P., Schulte-Schrepping, J., Blecher, R., Ulas, T., Squarzoni, P., Hoeffel, G., Coulpier, F., Siopi, E., David, F. S., Scholz, C., Shihui, F., Lum, J., Amoyo, A. A., Larbi, A., Poidinger, M., Buttgereit, A., Lledo, P.-M., Greter, M., Chan, J. K. Y., Amit, I., Beyer, M., Schultze, J. L., Schlitzer, A., Pettersson, S., Ginhoux, F., & Garel, S. (2018). Microbiome Influences Prenatal and Adult Microglia in a Sex-Specific Manner. *Cell, 172*(3), 500-516.e516.

Varol, D., Mildner, A., Blank, T., Shemer, A., Barashi, N., Yona, S., David, E., Boura-Halfon, S., Segal-Hayoun, Y., Chappell-Maor, L., Keren-Shaul, H., Leshkowitz, D., Hornstein, E., Fuhrmann, M., Amit, I., Maggio, N., Prinz, M., & Jung, S. (2017). Dicer Deficiency Differentially Impacts Microglia of the Developing and Adult Brain. *Immunity, 46*(6), 1030-1044.e1038.

Verdonk, F., Roux, P., Flamant, P., Fiette, L., Bozza, F. A., Simard, S., Lemaire, M., Plaud, B., Shorte, S. L., Sharshar, T., Chrétien, F., & Danckaert, A. (2016). Phenotypic clustering: a novel method for microglial morphology analysis. *J Neuroinflam, 13*(1), 153.

Weinhard, L., Neniskyte, U., Vadisiute, A., di Bartolomei, G., Aygün, N., Riviere, L., Zonfrillo, F., Dymecki, S., & Gross, C. (2018). Sexual dimorphism of microglia and synapses during mouse postnatal development. *Developmental neurobiology, 78*(6), 618-626.

Wendeln, A.-C., Degenhardt, K., Kaurani, L., Gertig, M., Ulas, T., Jain, G., Wagner, J., Häsler, L. M., Wild, K., Skodras, A., Blank, T., Staszewski, O., Datta, M., Centeno, T. P., Capece, V., Islam, M. R., Kerimoglu, C., Staufenbiel, M., Schultze, J. L., Beyer, M., Prinz, M., Jucker, M., Fischer, A., & Neher, J. J. (2018). Innate immune memory in the brain shapes neurological disease hallmarks. *Nature, 556*(7701), 332-338.

Wohleb, E. S., Fenn, A. M., Pacenta, A. M., Powell, N. D., Sheridan, J. F., & Godbout, J. P. (2012). Peripheral innate immune challenge exaggerated microglia activation, increased the number of inflammatory CNS macrophages, and prolonged social withdrawal in socially defeated mice. *Psychoneuroendocrinology, 37*(9), 1491-1505.

Wolf, Y., Yona, S., Kim, K.-W., & Jung, S. (2013). Microglia, seen from the CX3CR1 angle. *Front. Cell. Neurosci., 7*, 26.

Yanguas-Casás, N. (2020). Physiological sex differences in microglia and their relevance in neurological disorders. *Neuroimmunology and Neuroinflammation, 7*, 1-10.

Yirmiya, R. (1996). Endotoxin produces a depressive-like episode in rats. *Brain Research, 711*(1-2), 163-174.

Yona, S., Kim, K.-W., Wolf, Y., Mildner, A., Varol, D., Breker, M., Strauss-Ayali, D., Viukov, S., Guilliams, M., Misharin, A., Hume, D. A., Perlman, H., Malissen, B., Zelzer, E., & Jung, S. (2013). Fate mapping reveals origins and dynamics of monocytes and tissue macrophages under homeostasis. *Immunity, 38*(1), 79-91.

Zhang, L., Guadarrama, L., Corona-Morales, A. A., Vega-Gonzalez, A., Rocha, L., & Escobar, A. (2006). Rats subjected to extended L-tryptophan restriction during early postnatal stage exhibit anxious-depressive features and structural changes. *J Neuropathol Exp Neurol, 65*(6), 562-570.

Zhu, C.-B., Lindler, K. M., Owens, A. W., Daws, L. C., Blakely, R. D., & Hewlett, W. A. (2010). Interleukin-1 Receptor Activation by Systemic Lipopolysaccharide Induces Behavioral Despair Linked to MAPK Regulation of CNS Serotonin Transporters. *Neuropsychopharmacolgy, 35*(13), 2510-2520.

Zoratto, F., Fiore, M., Ali, S. F., Laviola, G., & Macrì, S. (2013). Neonatal tryptophan depletion and corticosterone supplementation modify emotional responses in adult male mice. *Psychoneuroendocrinology, 38*(1), 24-39.

*Figure Legends*

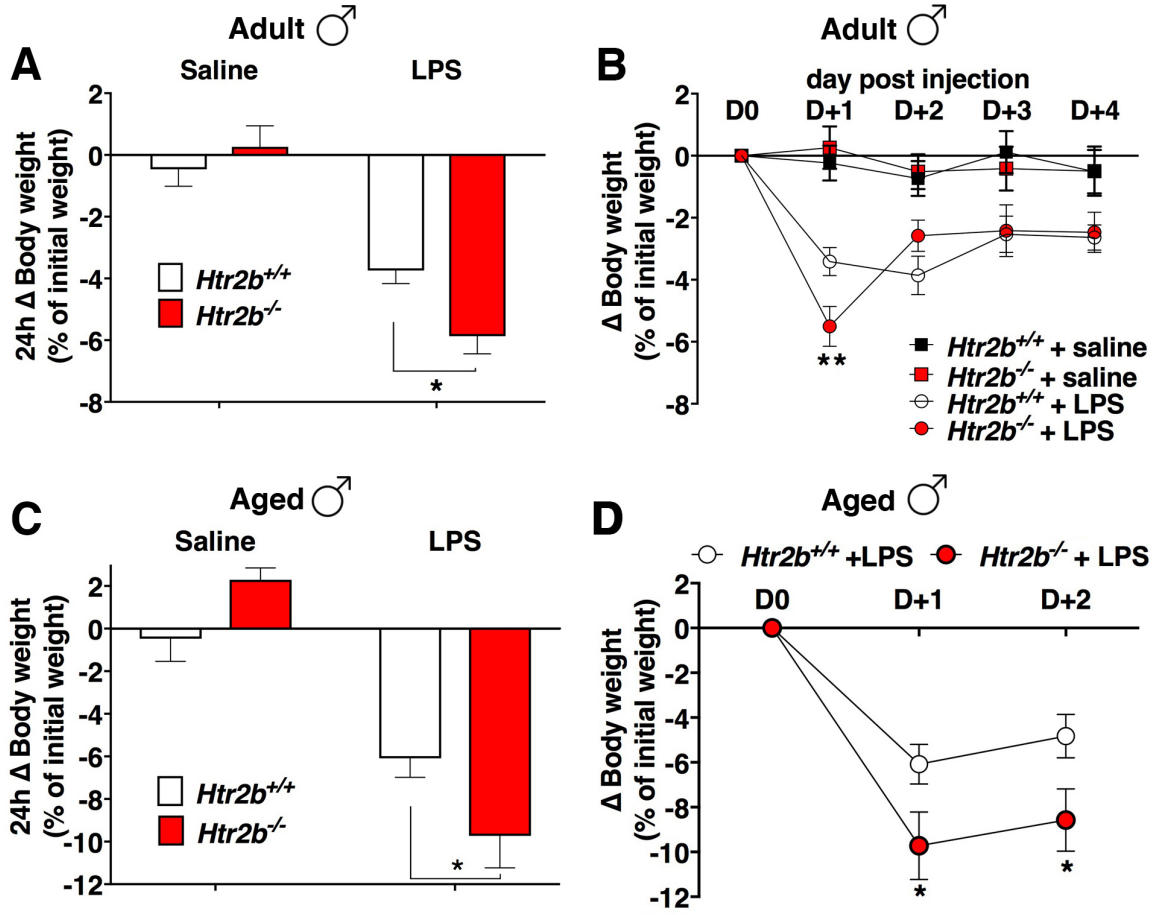


**Figure 1 : Weight loss after LPS injection is exacerbated in the absence of *Htr2b* in adult and aged male mice**. (**A**) Weight loss 24h after Saline or LPS injection, in adult male mice. Two-way ANOVA indicated a significant interaction between genotype (*Htr2b*$^{+/+}$: white bars; *Htr2b*$^{-/-}$: red bars) and treatment ($F_{1,64}$ = 6.63, *p=0.0124*) and post-hoc Bonferroni's tests indicated a significant difference between LPS groups (*p=0.016). *Htr2b*$^{+/+}$: n=18 (Saline) and 21 (LPS), *Htr2b*$^{-/-}$: n=15 (Saline) and 14 (LPS). (**B**) Time-course of weight variation in adult males (*Htr2b*$^{+/+}$: black or white symbols, *Htr2b*$^{-/-}$: red symbols) after LPS (circles) or saline (squares) injection. Two-way ANOVA with repeated measures (RM) from D0 to D+2 indicated a significant interaction between time and genotype ($F_{2,72}$ = 9.72, *p=0.0002*) and post hoc Bonferroni's multiple comparison of LPS groups indicated a stronger weight loss in *Htr2b*$^{-/-}$ than in *Htr2b*$^{+/+}$ mice at D+1: **p=0.0067. n=23 *Htr2b*$^{+/+}$+LPS, n=15 *Htr2b*$^{-/-}$+LPS, n=16 *Htr2b*$^{+/+}$+LPS, n=15 *Htr2b*$^{-/-}$+LPS. (**C**) Weight loss 24h after Saline or LPS injection, in aged male mice. Two-way ANOVA indicated a significant genotype x treatment interaction ($F_{1,34}$ = 7.96, *p=0.0079*) and post-hoc Bonferroni's tests indicated a significant difference between LPS groups (*p=0.037). *Htr2b*$^{+/+}$: n=9 (Saline) and 12 (LPS), *Htr2b*$^{-/-}$: n=7 (Saline) and 10 (LPS). (**D**) Time-course of weight variation in aged males after LPS injection. Two-way ANOVA-RM indicated a significant interaction between genotype and time ($F_{2,40}$ = 4.27, *p=0.021*), Bonferroni's post-hoc test of LPS groups indicated a significant difference between genotypes at D+1: *p=0.029, and D+2: *p=0.024. n=12 *Htr2b*$^{+/+}$ and 10 *Htr2b*$^{-/-}$. Data were collected from two to four independent experiments. Means ± SEM.

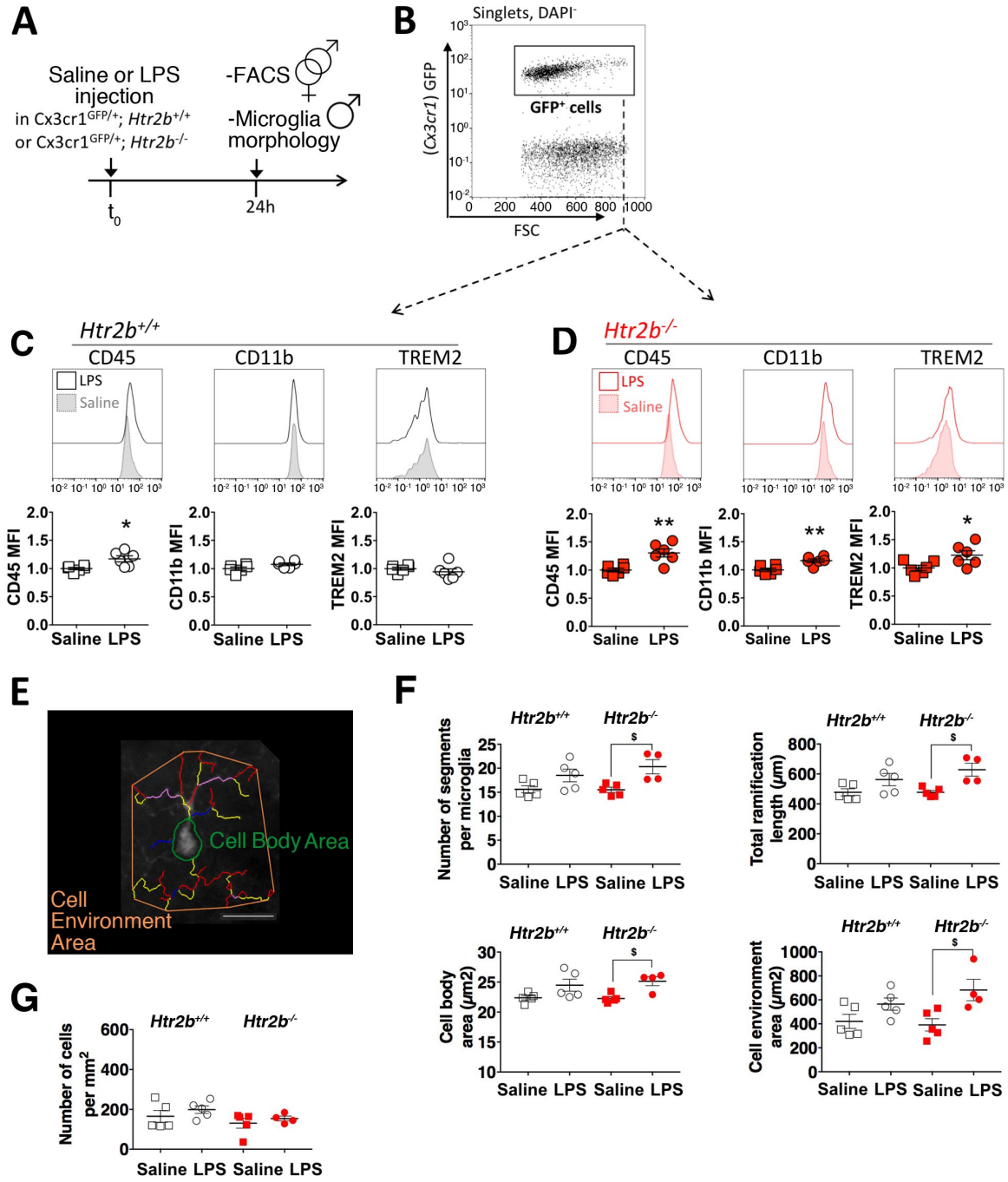


**Figure 2: Microglial changes after a peripheral inflammation are exacerbated in the absence of *Htr2b*.** **(A)** Timeline for LPS or Saline injection and FACS (males and females together) or microglia morphology (only males) analyses. (**B-D**) Flow cytometry on whole brain. (**B**) Example of FSC-GFP dotplot of a brain cell suspension from a *Cx3cr1*$^{GFP/+}$ mouse (after doublet and dead cells exclusion), to show the GFP$^{+}$ population ("GFP$^{+}$ cells") gated for the MFI measures shown in **C** and **D**. (**C, D**) Histograms showing MFIs of surface CD45, CD11b or TREM2 in the GFP$^{+}$ cells and relative quantification in Saline and LPS conditions, in samples from *Cx3cr1*$^{GFP/+}$; *Htr2b*$^{+/+}$ (**C**) or *Cx3cr1*$^{GFP/+}$; *Htr2b*$^{-/-}$ (**D**) mice. For CD45: *p=0.021 and **p=0.006; for CD11b: **p=0.004; for TREM2: *p=0.04; unpaired t test with Welch's correction. N = 6 mice/condition. Means ± SEM. **(E-F)** Microglia morphology analysis in males, in the hippocampus. **(E)** Example of a microglia and its reconstruction. Connected but distinct microglial segments have different colors. The total ramification length is the sum of the lengths of these segments. The green line delineates the cell body area. The

orange line is the polygon delineating the cell environment area. Bar = 5 μm. (**F**) In males, microglia morphological parameters were significantly altered by LPS injection in *Htr2b*$^{-/-}$ (red symbols), but not in *Htr2b*$^{+/+}$ animals (white symbols). Kruskal-Wallis test and Dunn post hoc tests indicated a significant difference between LPS- and Saline-treated groups in *Htr2b*$^{-/-}$ mice for the number of segments ($^{\$}$p=0.013), for the total ramification length ($^{\$}$p=0.013), for the cell body area ($^{\$}$p=0.017) and for the cell environment area ($^{\$}$p=0.010). *Htr2b*$^{+/+}$: n=5 (Saline) and 5 (LPS); *Htr2b*$^{-/-}$: n=5 (Saline) and 4 (LPS). The value for each animal is calculated from 200 microglia on average. (**G**) No effect of treatment nor genotype on microglial cell density in males. Test and n: as in **(F)**.

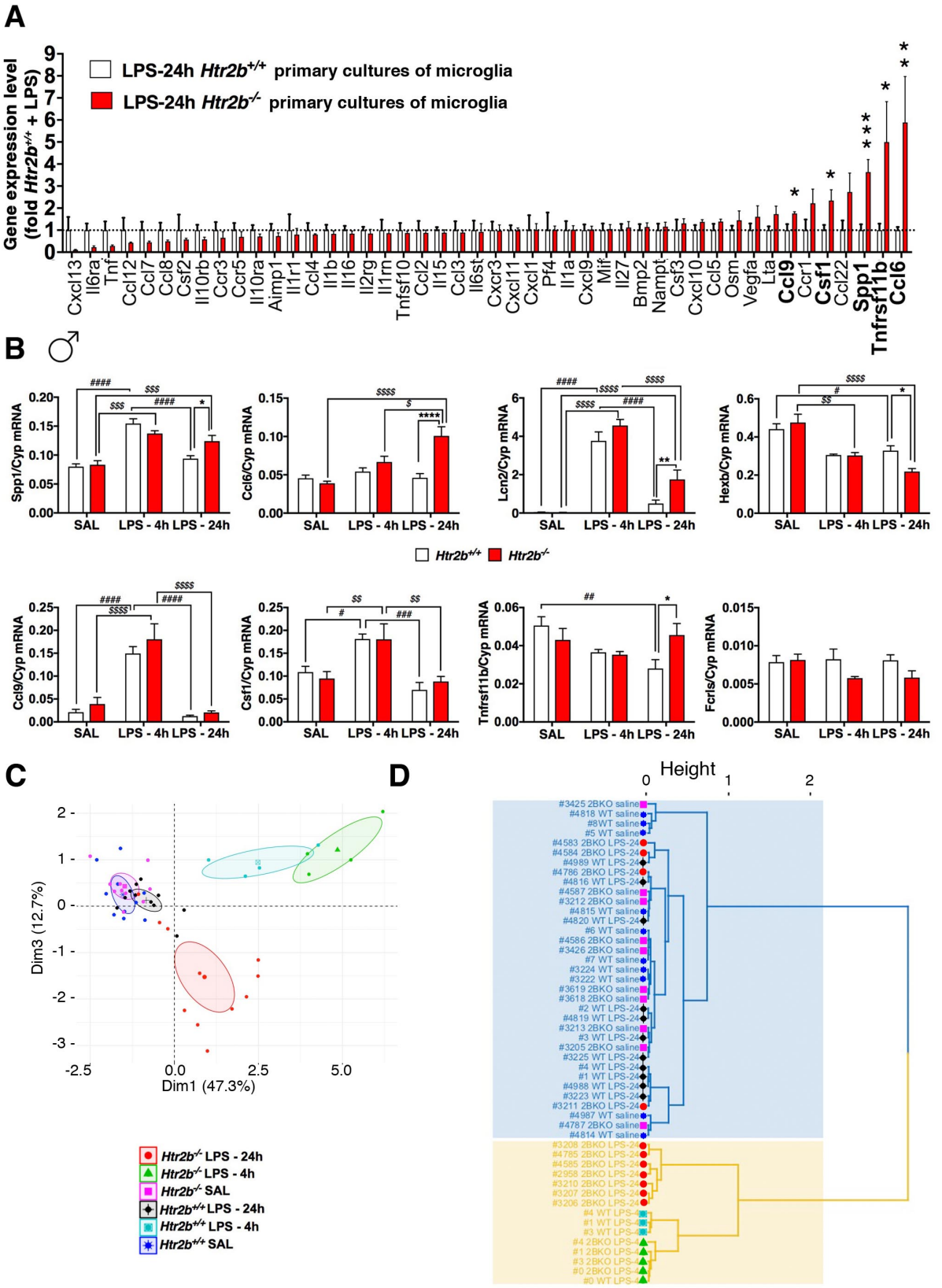


**Figure 3: Stronger LPS-induced microglial activation *in vitro* and prolonged neuroinflammation *in vivo* in adult male mice in the absence of *Htr2b*.** (**A**) Several inflammatory genes are overexpressed in LPS-treated microglial primary cultures from *Htr2b*$^{-/-}$ (red bars), compared to *Htr2b*$^{+/+}$ (white bars) pups. **p=0.006 *Ccl6*, *p=0.013 *Tnfrsf11b*, ***p=0.0004 *Spp1*, *p=0.017 *Csf1*, *p=0.030 *Ccl9*, multiple t test; n=4 independent cultures

per genotype (each culture is performed from a pool of male and female pups). Means ± SEM. (**B-D**) Analysis of gene expression in whole brain of male mice, in control condition (SAL: 24h after a saline injection) or 4 or 24h after a peripheral LPS injection. **(B)** Overall, significant differences between genotypes were observed by two-way ANOVA, only at 24h after LPS injection, for *Spp1* mRNA (genotype x treatment interaction $F_{2,43}$ = 4.125, *p=0.023*; Bonferroni's post-hoc *p=0.0065), for *Ccl6* mRNA (genotype x treatment interaction $F_{2,47}$ = 10.81, *p=0.0001*; Bonferroni's post-hoc ****p<0.0001), for *Lcn2* mRNA (genotype x treatment interaction $F_{2,49}$ = 3.522, *p=0.037*; Bonferroni's post-hoc **p=0.0031), and for *Hexb* mRNA (genotype x treatment interaction $F_{2,37}$ = 3.23, *p=0.050*; Bonferroni's post-hoc *p=0.0323). Other Bonferroni's post-hoc tests: $^{\$}$p<0.05, $^{\$\$}$p<0.01, $^{\$\$\$}$p<0.001, $^{\$\$\$\$}$p<0.0001 among *Htr2b*$^{-/-}$ groups and $^{\#}$p<0.05, $^{\#\#}$p<0.01, $^{\#\#\#}$p<0.001, $^{\#\#\#\#}$p<0.0001 among *Htr2b*$^{+/+}$ groups. *Htr2b*$^{+/+}$: n=8-14 (SAL), 3-4 (LPS-4h) and 8-11 (LPS-24h), *Htr2b*$^{-/-}$: n=3-10 (SAL), 4 (LPS-4h) and 8-12 (LPS-24h). Data pooled from at least four independent experiments. Means ± SEM. (**C**) PCA highlights the peculiar neuroinflammatory state of *Htr2b*$^{-/-}$ mice, 24h after LPS injection (red dots, barycenter symbol and ellipse), contrasting with that of *Htr2b*$^{+/+}$ mice at the same time-point (black dots, barycenter symbol and ellipse). **(D)** A hierarchical clustering partitions the samples in two groups (cluster 1 in blue, cluster 2 in yellow), showing that neuroinflammation in *Htr2b*$^{-/-}$ ("2B KO") mice 24h after LPS injection is close to acute neuroinflammation (LPS 4h), whereas in *Htr2b*$^{+/+}$ ("WT") mice, the situation 24h after LPS injection is close to the saline condition. Symbols as in (**C**).

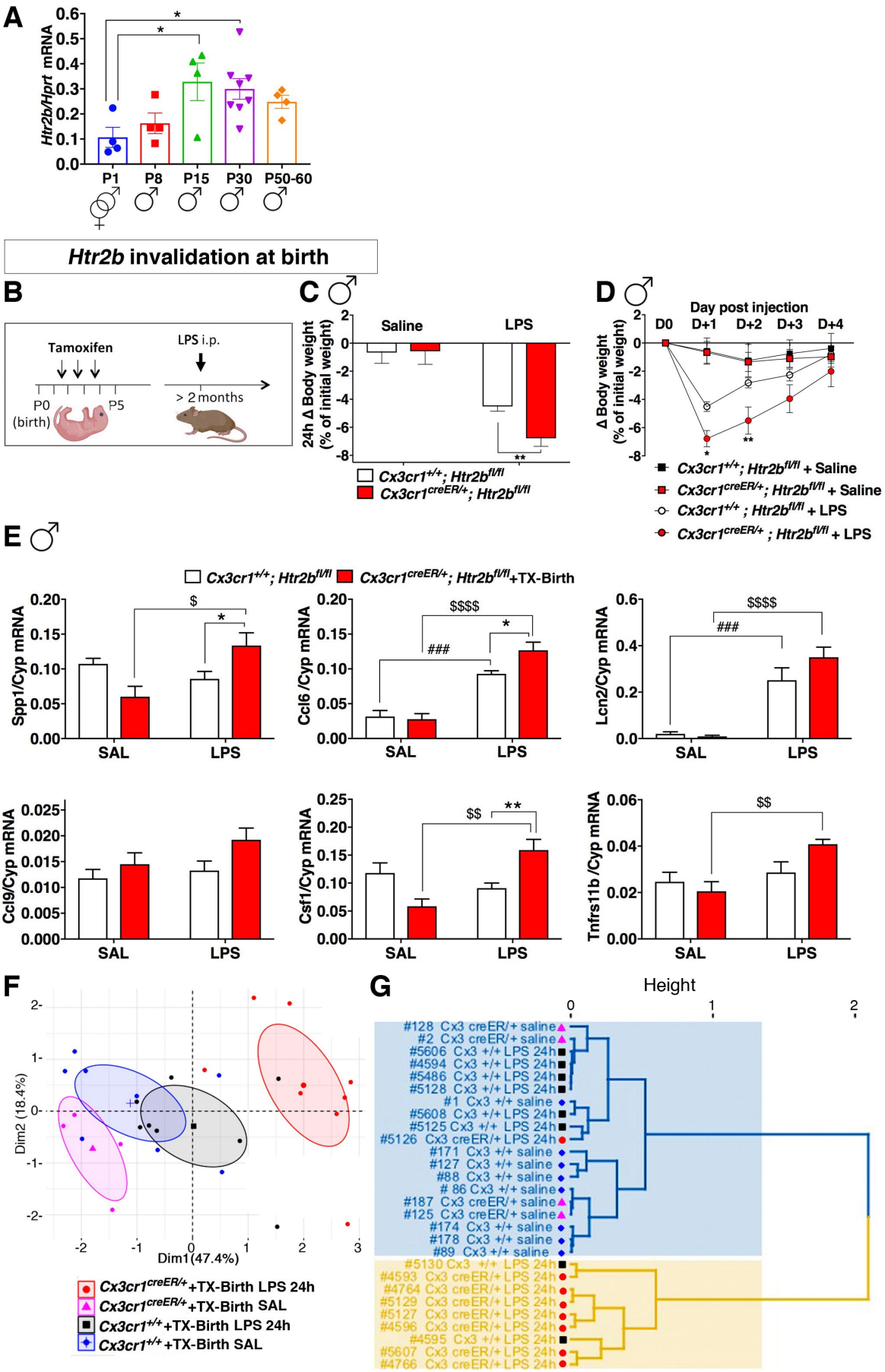
A
Htr2b/Hprt mRNA
P1
P8
P15
P30
P50-60
Htr2b invalidation at birth
B
Tamoxifen
LPS i.p.
P0 (birth)
P5
> 2 months
C
Saline
LPS
24h Δ Body weight (% of initial weight)
Cx3cr1+/+; Htr2bfl/fl
Cx3cr1creER/+; Htr2bfl/fl
D
Day post injection
D0
D+1
D+2
D+3
D+4
Δ Body weight (% of initial weight)
Cx3cr1+/+; Htr2bfl/fl + Saline
Cx3cr1creER/+; Htr2bfl/fl + Saline
Cx3cr1+/+ ; Htr2bfl/fl + LPS
Cx3cr1creER/+ ; Htr2bfl/fl + LPS
E
Cx3cr1+/+; Htr2bfl/fl
Cx3cr1creER/+; Htr2bfl/fl+TX-Birth
Spp1/Cyp mRNA
Ccl6 /Cyp mRNA
Lcn2/Cyp mRNA
Ccl9/Cyp mRNA
Csf1/Cyp mRNA
Tnfrs11b /Cyp mRNA
SAL
LPS
F
Dim2 (18.4%)
Dim1(47.4%)
Cx3cr1creER/+ +TX-Birth LPS 24h
Cx3cr1creER/+ +TX-Birth SAL
Cx3cr1+/+ +TX-Birth LPS 24h
Cx3cr1+/+ +TX-Birth SAL
G
Height
#128 Cx3 creER/+ saline
#2 Cx3 creER/+ saline
#5606 Cx3 +/+ LPS 24h
#4594 Cx3 +/+ LPS 24h
#5486 Cx3 +/+ LPS 24h
#5128 Cx3 +/+ LPS 24h
#1 Cx3 +/+ saline
#5608 Cx3 +/+ LPS 24h
#5125 Cx3 +/+ LPS 24h
#5126 Cx3 creER/+ LPS 24h
#171 Cx3 +/+ saline
#127 Cx3 +/+ saline
#88 Cx3 +/+ saline
# 86 Cx3 +/+ saline
#187 Cx3 creER/+ saline
#125 Cx3 creER/+ saline
#174 Cx3 +/+ saline
#178 Cx3 +/+ saline
#89 Cx3 +/+ saline
#5130 Cx3 +/+ LPS 24h
#4593 Cx3 creER/+ LPS 24h
#4764 Cx3 creER/+ LPS 24h
#5129 Cx3 creER/+ LPS 24h
#5127 Cx3 creER/+ LPS 24h
#4596 Cx3 creER/+ LPS 24h
#4595 Cx3 +/+ LPS 24h
#5607 Cx3 creER/+ LPS 24h
#4766 Cx3 creER/+ LPS 24h

**Figure 4: Invalidation of *Htr2b* selectively in microglia since birth is sufficient to exacerbate LPS-induced weight loss and neuroinflammation in adult male mice**. (**A**) Time-course of *Htr2b* mRNA expression in microglia during postnatal development. One-way ANOVA showed an effect of age ($F_{4, 19} = 3.52$ *p=0.0261*); Bonferroni's post-hoc tests revealed significant difference between P1 and P15 (*p=0.0305) and between P1 and P30 (*p=0.0291); n=4-8 males, except at P1 (n=4 pools of pups of undetermined sex). (**B**) Timeline of tamoxifen treatment for early *Htr2b* microglial invalidation, and LPS injection. (**C**) Weight loss 24h after Saline or LPS injection in male mice. Two-way ANOVA showed a main effect of treatment ($F_{1,43} = 66.12$, *p<0.0001*) and post-hoc Bonferroni's post hoc tests revealed a significant difference between LPS groups (**p=0.0082). *Cx3cr1*$^{+/+}$*; Htr2b*$^{fl/fl}$ (white bars): n=7 (SAL) and 23 (LPS); *Cx3cr1*$^{CreERT2/+}$*; Htr2b*$^{fl/fl}$ (red bars): n=8 (Saline) and 9 (LPS). (**D**) Time-course of weight variation in male mice after LPS (circles) or Saline (squares) injection. Two-way ANOVA with repeated measures (RM) showed a genotype x time interaction ($F_{4,120} = 3.15$, *p=0.017*) and post-hoc Bonferroni's tests between LPS groups indicated a stronger weight loss in *Cx3cr1*$^{CreERT2/+}$*; Htr2b*$^{fl/fl}$ (red circles) than in *Cx3cr1*$^{+/+}$*; Htr2b*$^{fl/fl}$ (white circles) mice, at D+1 (*p=0.020) and D+2 (**p=0.004). n: as in (**C**). (**E-G**) Analysis of gene expression in whole brain of male mice, 24h after LPS or saline (SAL) injection. (**E**) Overall, significant differences between genotypes were observed after LPS injection, by two-way ANOVA, for *Spp1* mRNA (genotype x treatment interaction $F_{1,24} = 11.06$, *p=0.0028*; Bonferroni's post-hoc *p=0.030), for *Ccl6* mRNA (main effect of treatment $F_{1,21} = 70.12$, *p<0.0001*; Bonferroni's post-hoc *p=0.031), and for *Csf1* mRNA (genotype x treatment interaction $F_{1,24} = 13.81$, *p=0.001*; Bonferroni's post-hoc **p=0.0090). Other Bonferroni's post-hoc tests: $^{\$}$p<0.05, $^{\$\$}$p<0.01, $^{\$\$\$\$}$p<0.0001 among *Cx3cr1*$^{CreERT2/+}$*; Htr2b*$^{fl/fl}$ groups, and $^{\#\#\#}$p<0.001 among *Cx3cr1*$^{+/+}$*; Htr2b*$^{fl/fl}$ groups. *Cx3cr1*$^{+/+}$*; Htr2b*$^{fl/fl}$: n=7-8 (SAL) and 6-8 (LPS), *Cx3cr1*$^{CreERT2/+}$*; Htr2b*$^{fl/fl}$: n=4 (SAL) and 7-8 (LPS). Data pooled from at least four independent experiments. (**F**) PCA highlights the peculiar neuroinflammatory response of animals invalidated for *Htr2b* at birth ("*Cx3cr1*$^{creER/+}$+TX-Birth -LPS 24", red dots, barycenter symbol and ellipse). **(G)** A hierarchical clustering partitions the samples in two groups (cluster 1 in blue, cluster 2 in yellow), showing that 24h after LPS, neuroinflammation in animals invalidated for *Htr2b* at birth ("Cx3 creER/+") has not resumed as well as in their control littermates ("Cx3 +/+"). Symbols as in (**F**). **(C-E)** Means ± SEM.

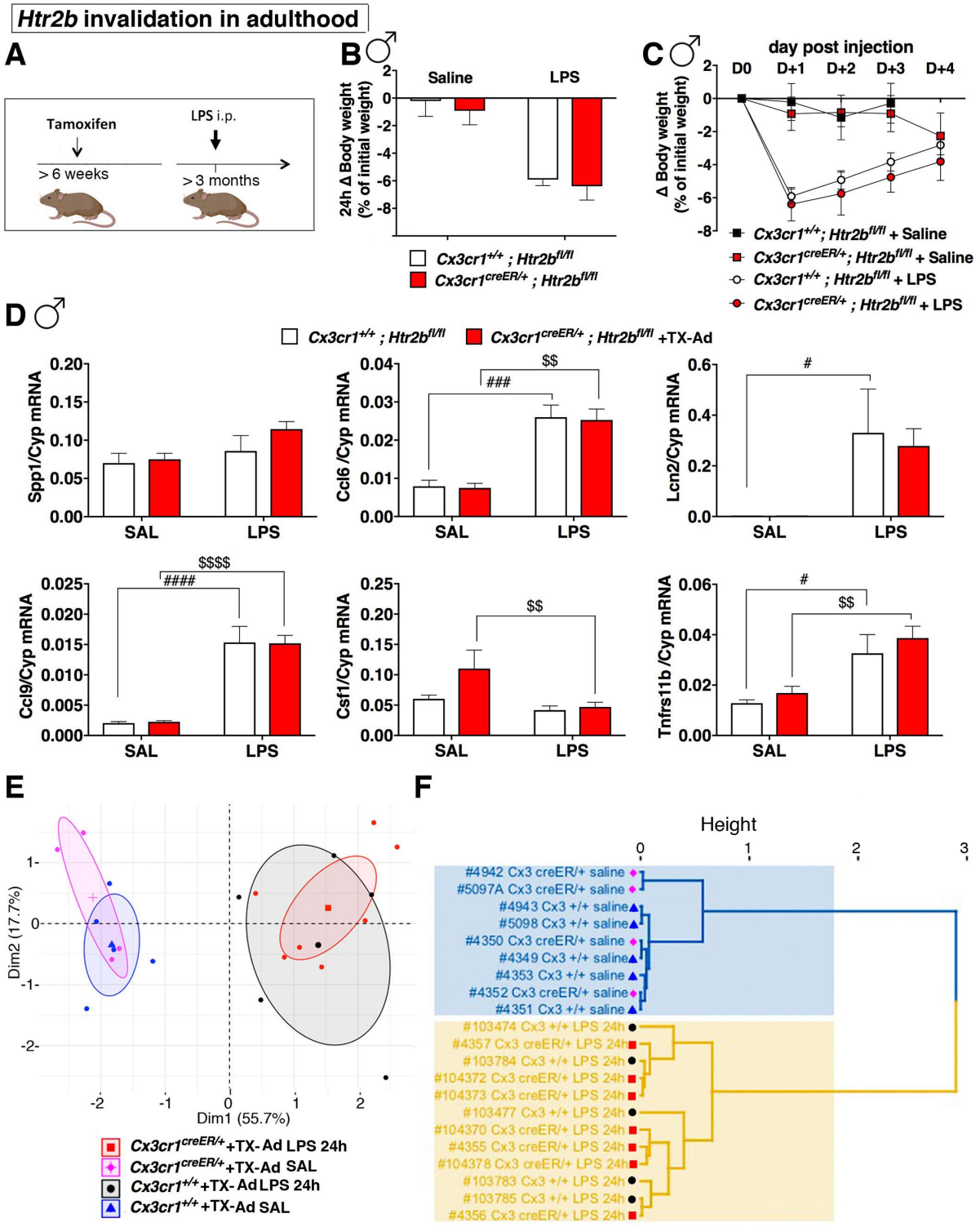


**Figure 5: Invalidation of *Htr2b* in microglia in adulthood does not sensitize to the effects of LPS in male mice**. (**A**) Timeline of tamoxifen treatment for *Htr2b* invalidation in microglia in adulthood, and LPS injection. (**B**) Weight loss 24h after saline or LPS injection in male mice. Two-way ANOVA showed no difference between genotypes after LPS injection. *Cx3cr1*$^{+/+}$*; Htr2b*$^{fl/fl}$ (white bars): n=7 (Saline) and 15 (LPS), *Cx3cr1*$^{CreERT2/+}$*; Htr2b*$^{fl/fl}$ (red bars): n=5 (Saline) and 8 (LPS). (**C**) Time-course of weight variation in male mice after LPS (circles) or saline (squares) injection. Two-way ANOVA-RM from D0 to D+3 showed no difference between genotypes after LPS injection. n: as in (**B**). (**D-F**) Analysis of gene expression in whole brain of male mice, 24h after LPS or saline (SAL) injection. (**D**) Overall, no significant

difference between genotypes was found (two-way ANOVA). Other Bonferroni's post-hoc comparisons: $^{\$\$}p<0.01$, $^{\$\$\$\$}p<0.0001$ among *Cx3cr1*$^{CreERT2/+}$*; Htr2b*$^{fl/fl}$ groups and $^{\#}p<0.05$, $^{\#\#\#}p<0.001$ among *Cx3cr1*$^{+/+}$*; Htr2b*$^{fl/fl}$ groups. *Cx3cr1*$^{+/+}$*; Htr2b*$^{fl/fl}$: n=4-5 (SAL) and 4-5 (LPS) groups, *Cx3cr1*$^{CreERT2/+}$*; Htr2b*$^{fl/fl}$: n=3-4 (SAL) and 6-7 (LPS). Data pooled from four independent experiments. (**E**) PCA and (**F**) hierarchical clustering show that 24h after LPS treatment, the neuroinflammatory state of animals invalidated for *Htr2b* in adulthood (quoted "*Cx3cr1*$^{creER/+}$ +TX-Ad" or "Cx3 creER/+", red dots, barycenter symbol and ellipse), does not distinguish them from control littermates ("*Cx3cr1*$^{+/+}$ +TX-Ad" or "Cx3+/+", black dots, barycenter symbol and ellipse). **(B-D)** Means ± SEM.

**The serotonin 2B receptor is required in neonatal microglia to limit neuroinflammation and sickness behavior in adulthood.**

Béchade, C[1,2,3], D'Andrea, I[1,2,3], Etienne, F[1,2,3,*], Verdonk, F[4], Moutkine, I[1,2,3], Banas, SM[1,2,3], Kolodziejczak, M[1,2,3,8], Diaz, SL[1,2,3,5], Parkhurst, CN[6,7], Gan W-B[6], Maroteaux, L[1,2,3], Roumier, A[1,2,3]

## Supplementary methods

### Cytokines measurement (for Fig. S6)

4h or 24h after injection with LPS or 24h after saline injection, adult male mice were anesthetized with pentobarbital and blood samples were taken by intracardiac puncture in microvette 500LH-gel tubes (Sarstedt). Plasma was collected by centrifugation at 2,000 g 10 mins and stored at -80°C until assay. Plasma concentrations of Lcn2, Spp1 and Ccl6 were determined by enzyme-linked immunosorbent assay (ELISA) (R&D systems).

### Microglia purification to assess the cell-specificity of *Htr2b* recombination (for Fig. S7)

For cell sorting, the procedure to prepare the cell suspension was the same as for flow cytometry. Then, the suspension was incubated with anti-CD11b antibody coupled to magnetic beads (Miltenyi Biotec). Purification of microglia (CD11b-labeled cells) was performed by magnetic separation according to the manufacturer's instructions (Miltenyi Biotec). The non-microglia fraction corresponds to the non-labeled cells, which flowed in the flow-through. Purity of the fractions (>90%) was systematically controlled by flow cytometry.

### Supplementary Figures:

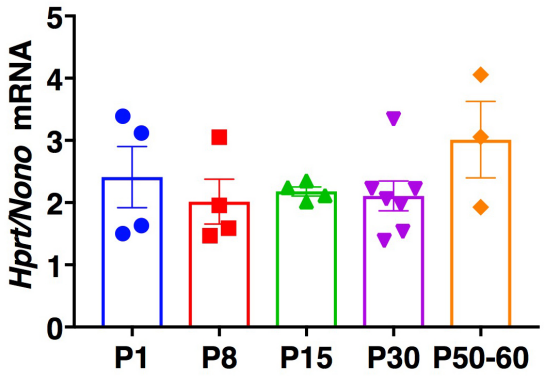


**Figure S1: Comparison of *Hprt* expression to that of *Nono* during development**
Quantification of microglia *Hprt* mRNA expression was performed using TaqMan (Bio-Rad) and the PrimePCR probe assays for *Hprt* (qMmuCID0005679) and *Nono* (qMmuCED0040697) as reference gene at different postnatal days (P1 to P60). The results were processed according to the $2^{-\Delta\Delta Ct}$ method and showed no significant change in expression as analyzed by one-way ANOVA.

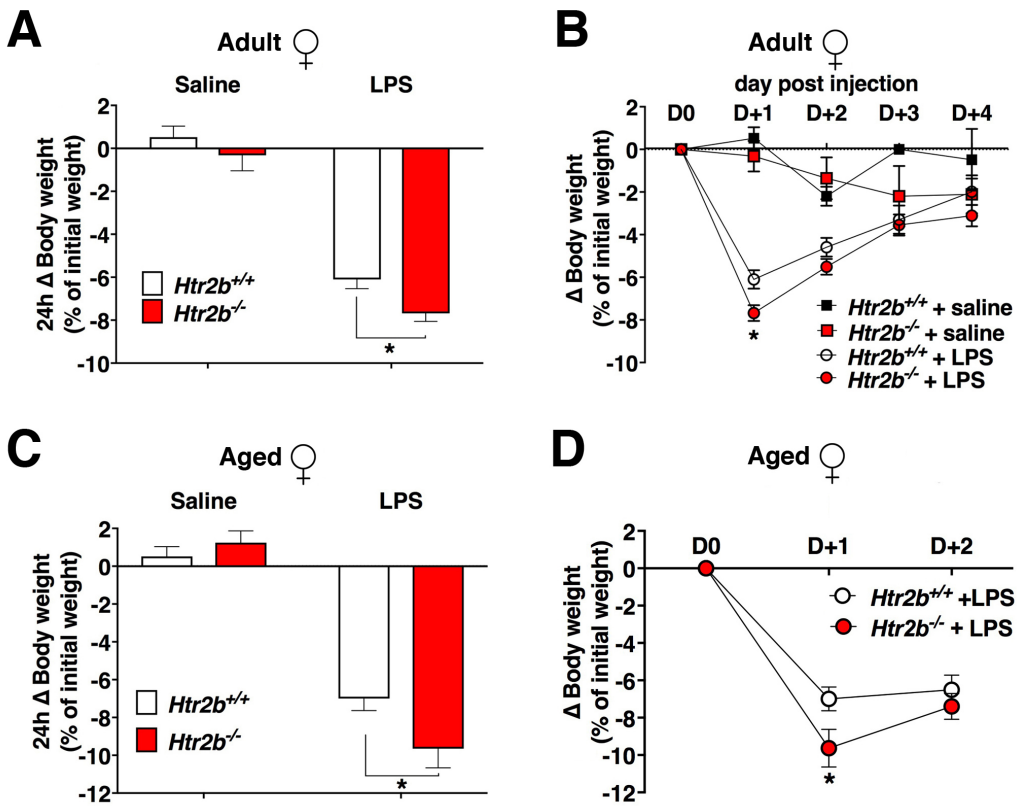


**Figure S2: Time-course of weight variation induced by peripheral inflammation in *Htr2b*$^{+/+}$ (black or white symbols) and *Htr2b*$^{-/-}$ (red symbols) female mice, adult (A-B) or aged (C-D).** (**A**) In adult females, two-way ANOVA indicated a main effect of treatment ($F_{1,58}$ = 123.6, *p<0.0001*) and post-hoc Bonferroni's tests indicated a significant difference between LPS groups (*p=0.039). *Htr2b*$^{+/+}$: n= 5 (Saline) and 16 (LPS), *Htr2b*$^{-/-}$: n=15 (Saline) and 26 *Htr2b*$^{-/-}$(LPS). (**B**) Weight loss and recovery in adult females after LPS or saline injection. Two-way ANOVA-RM from D0 to D+2 indicated a significant interaction between time and genotype ($F_{2,80}$ = 3.23, *p=0.045*) and post hoc Bonferroni's multiple comparison of LPS groups indicated a stronger weight loss in *Htr2b*$^{-/-}$ than in *Htr2b*$^{+/+}$ mice at D+1: **p=0.0036; n=16 *Htr2b*$^{+/+}$+LPS, n=24 *Htr2b*$^{-/-}$+LPS, n=5 *Htr2b*$^{+/+}$+LPS, n=12 *Htr2b*$^{-/-}$+LPS. Data collected from at least 3 independent experiments. Means ± SEM. (**C**) In aged females, two-way ANOVA indicated a significant effect of treatment ($F_{1,31}$ = 111.6, *p<0.0001*) and post-hoc Bonferroni's tests indicated a significant difference between LPS groups (*p=0.033). *Htr2b*$^{+/+}$: n=5 (Saline) and 11 (LPS), *Htr2b*$^{-/-}$:8 (Saline) and 11 (LPS). (**D**) Weight loss and recovery in aged females after LPS injection. Two-way ANOVA-RM indicated a significant interaction between genotype and time ($F_{2,40}$ = 3.36, *p=0.045*), Bonferroni's post-hoc test of LPS groups indicated a significant difference between genotypes at D+1: *p=0.017 (n=11 *Htr2b*$^{+/+}$ and 11 *Htr2b*$^{-/-}$). Data collected from two to four independent experiments. Means ± SEM.

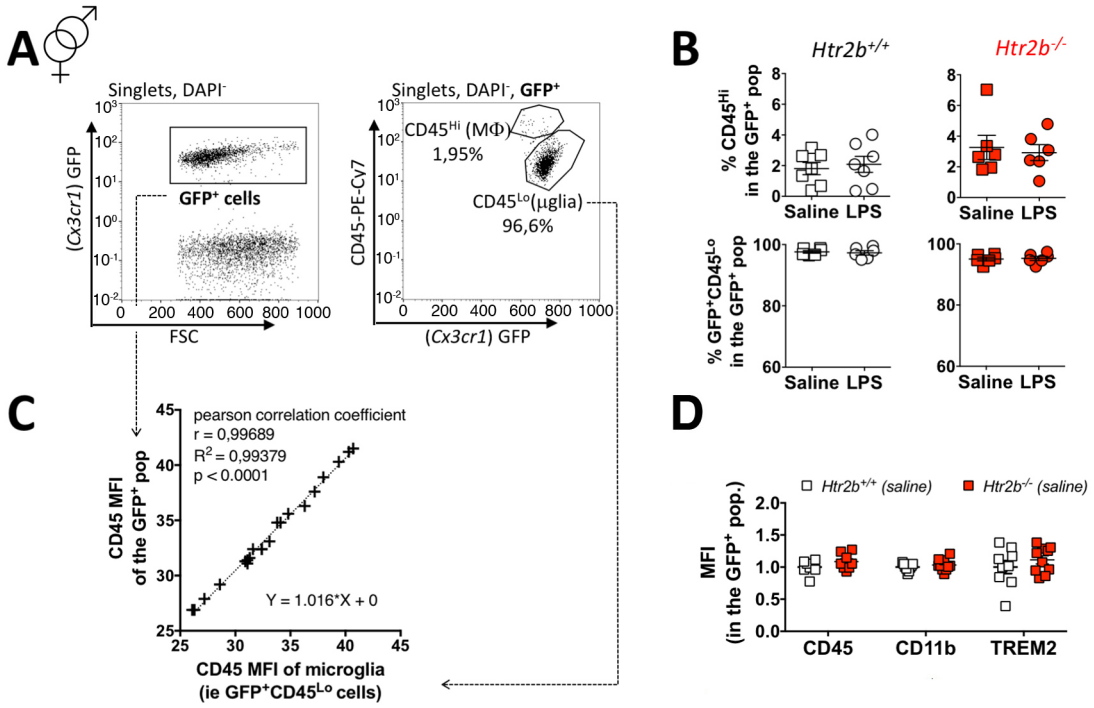


**Figure S3: Flow cytometry-based analysis of the brain myeloid cells. (A)** In the whole brain, labeling of CD45 shows that the $GFP^+$ (i.e. Cx3cr1- expressing) population is composed mainly of $GFP^+CD45^{Lo}$ cells (i.e. microglia), and of a small subset of $GFP^+CD45^{Hi}$ cells (i.e. monocytes/macrophages). (**B**) The percentage of these two subpopulations among the whole $GFP^+$ population does not vary after LPS injection, neither in *Htr2b*$^{+/+}$ nor *Htr2b*$^{-/-}$ genotype, indicating that there is no significant infiltration of peripheral myeloid cells at this dose of LPS and time-point. (**C**) The MFI value for CD45 labeling in a whole $GFP^+$ population is strongly correlated to the MFI value in its $GFP^+CD45^{Lo}$ subpopulation, which represents microglia and from which infiltrated monocytes and macrophages ($GFP^+CD45^{Hi}$) are excluded. Moreover, measuring CD45 MFI in the whole $GFP^+$ population overestimates the CD45 MFI of microglia ($GFP^+CD45^{Lo}$) on average by only 1.016 fold; n=21 animals, representative of all the genotype x treatment conditions. (**D**) Surface expression of CD45, CD11b and TREM2 in the myeloid ($GFP^+$) brain cells is not modified in the absence of *Htr2b* in basal condition (i.e. 24h after a saline injection), in adult mice. Unpaired t-test; n=6-10 mice, indifferently male or female, for each condition. Means ± SEM.

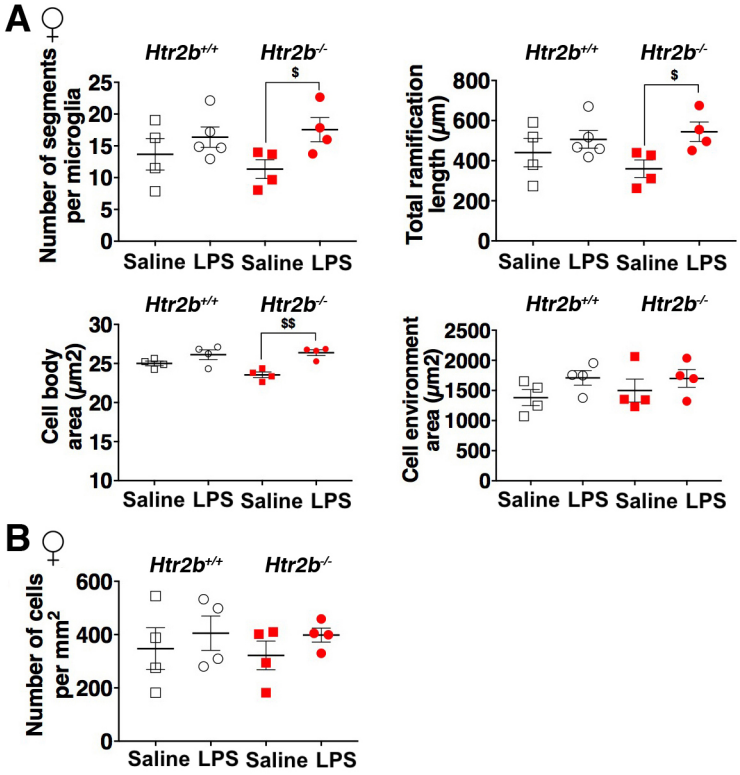


**Figure S4: Morphological alterations of microglia in the hippocampus of *Htr2b*$^{-/-}$ female mice in response to peripheral LPS injection**. (**A**) Kruskal-Wallis test and Dunn post hoc tests indicated a significant difference in *Htr2b*$^{-/-}$ female mice between LPS- and Saline-treated groups, 24h after the injection, for the number of segments ($^{\$}$p=0.036), the total ramification length ($^{\$}$p=0.021), and the cell body area, ($^{\$\$}$p=0.006), but not for the cell environment area. *Htr2b*$^{+/+}$: n=4 (Saline) and 5 (LPS), *Htr2b*$^{-/-}$: n=4 (Saline) and 4 (LPS). The value for each animal is calculated from 200 microglia on average. (**B**) No effect of treatment nor genotype on microglial cell density in females. Test and n: as in **(A).**

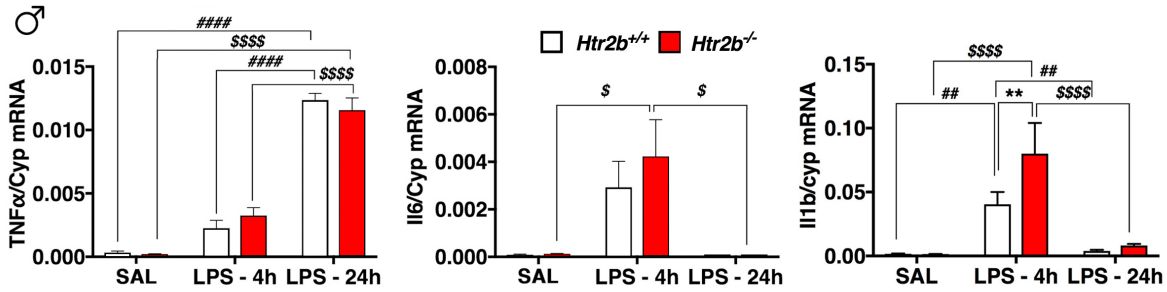


**Figure S5: Analysis of brain inflammatory markers in the absence of *Htr2b* in adult males.** Classical markers of LPS-induced neuroinflammation are not modified at 24h by the absence of *Htr2b* in adult males. No significant difference between genotypes, *Htr2b*$^{-/-}$ (red bars) compared to *Htr2b*$^{+/+}$ (white bars), was observed 24h after LPS injection for TNFα mRNA, (two-way ANOVA no interaction between genotype and treatment time $F_{2,31} = 0.527$, *p=0.595*; n=4-11 mice), nor for Il6 mRNA (no interaction between genotype and treatment time $F_{2,17} = 0.426$, *p=0.66*; n= 3-4 mice). A significant difference between genotypes was observed only at 4h after LPS injection for Il1β mRNA (two-way ANOVA interaction between genotype and treatment time $F_{2,36} = 5.34$, *p=0.0093*; Bonferroni's post-hoc *p=0.0094; n=4-10 mice). Other post-hoc comparisons revealing significant differences are shown $^{\$}$p<0.05, $^{\$\$\$\$}$p<0.0001 between *Htr2b*$^{-/-}$ time or treatment and $^{\#\#\#\#}$p<0.0001 between *Htr2b*$^{+/+}$ time or treatment. Number of animals (adult males) for TNFα, Il6, and Il1β, respectively: *Htr2b*$^{+/+}$ n=4-4-10 for SAL, n=11-4-7 for LPS-24h groups, n=4-4-4 for LPS-4h; *Htr2b*$^{-/-}$ n=3-3-10 for SAL, n=11-4-7 for LPS-24h groups, n=4-4-4 for LPS-4h. Means ± SEM.

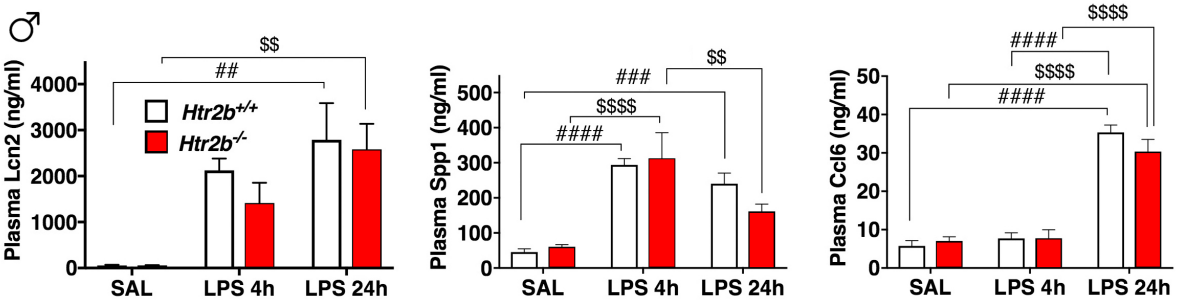


**Figure S6: Analysis of plasmatic levels of Lcn2, Spp1 and Ccl6 in the absence of *Htr2b* in adult males.** Plasma samples were prepared 4 and 24h after a peripheral LPS injection, or in control (24h after a saline-SAL injection) condition. The effect of treatment was significant for the three cytokines but no significant difference between genotypes, *Htr2b*$^{-/-}$ (red bars) compared to *Htr2b*$^{+/+}$ (white bars), was observed in any condition (24h after saline or 4h or 24h after LPS injection). For Lcn2, two-way ANOVA simple effect of treatment $F_{2,32} = 77.9$, *p=0.0002*; for Spp1, two-way ANOVA simple effect of treatment $F_{2,34} = 30.89$, *p=<0.0001*; for Ccl6, two-way ANOVA simple effect of treatment $F_{2,33} = 102.6$, *p=<0.0001*. Other post-hoc comparisons revealing significant differences are $^{\$\$}$p<0.01, $^{\$\$\$\$}$p<0.0001 among *Htr2b*$^{-/-}$ groups and $^{\#\#}$p<0.01, $^{\#\#\#}$p<0.001, $^{\#\#\#\#}$p<0.0001 among *Htr2b*$^{+/+}$ groups. Number of animals (adult males) for Lcn2, Spp1 and Ccl6, respectively: *Htr2b*$^{+/+}$ n=6-6-6 for SAL, n=8-8-8 for LPS-24h groups, n=5-6-5 for LPS-4h; *Htr2b*$^{-/-}$ n=5-6-7 for SAL, n=9-9-8 for LPS-24h groups, n=5-5-5 for LPS-4h. Means ± SEM.

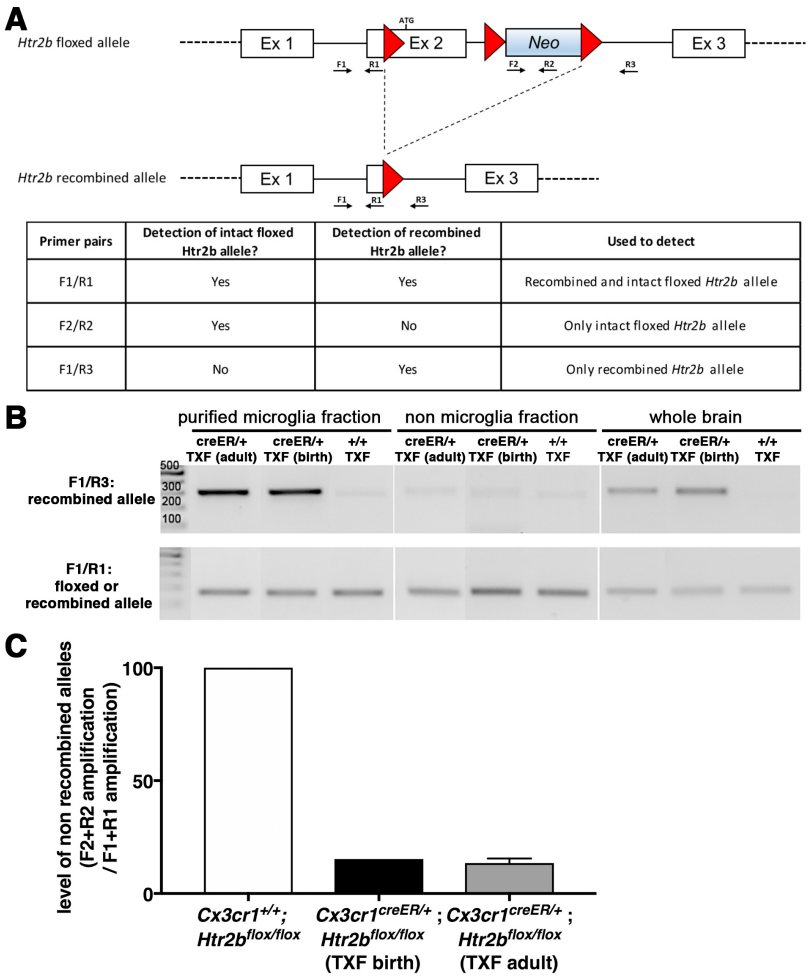


| Primer pairs | Detection of intact floxed Htr2b allele? | Detection of recombined Htr2b allele? | Used to detect |
|---|---|---|---|
| F1/R1 | Yes | Yes | Recombined and intact floxed *Htr2b* allele |
| F2/R2 | Yes | No | Only intact floxed *Htr2b* allele |
| F1/R3 | No | Yes | Only recombined *Htr2b* allele |

**Figure S7: Recombination in *Cx3cr1*$^{CreERT2/+}$; *Htr2b*$^{fl/fl}$ mice.** (**A**) Top: Schematic of the *Htr2b* locus in *Htr2b*$^{fl/fl}$ mice, before and after recombination, and position of the primers used. Bottom: combinations of primers used to detect the recombined and/or intact floxed *Htr2b* allele. Sequences are indicated in **Table 2**. (**B**) PCR to assess the specificity of recombination in microglia. Microglia and non-microglia fractions were purified by magnetic cell sorting (See Supplementary Methods) from adult *Cx3cr1*$^{+/+}$*; Htr2b*$^{fl/fl}$ and *Cx3cr1*$^{CreERT2/+}$*; Htr2b*$^{fl/fl}$ mice, all treated with tamoxifen at birth or in adulthood. Cells were lysed, DNA was purified, and PCR amplifications were performed to detect recombined (F1+R3 pair of primers) and intact (F1+R1 pair) loci. Only microglia bore the recombined allele, assessing the cell-specificity of the recombination, and no recombination was found in *Cx3cr1*$^{+/+}$; *Htr2b*$^{fl/fl}$, assessing the Cre-dependence of the recombination. (**C**) Quantitative PCR was performed on the DNA of microglia fractions, to assess the efficiency of recombination. To this aim, we used a primer pair that amplifies only the non-recombined locus (F2+R2), and F1+R1 pair for the internal reference. The level of *Htr2b* recombination in the microglia fraction of animals was determined with the $2^{-\Delta Ct}$ method using, for normalization, the level of the non-recombined allele in *Cx3cr1*$^{+/+}$; *Htr2b*$^{fl/fl}$ mice, which by nature (and as checked in B) cannot recombine. Similar decreases were observed in *Cx3cr1*$^{CreERT2/+}$*; Htr2b*$^{fl/fl}$ mice treated with tamoxifen at birth or in adulthood (>85%).

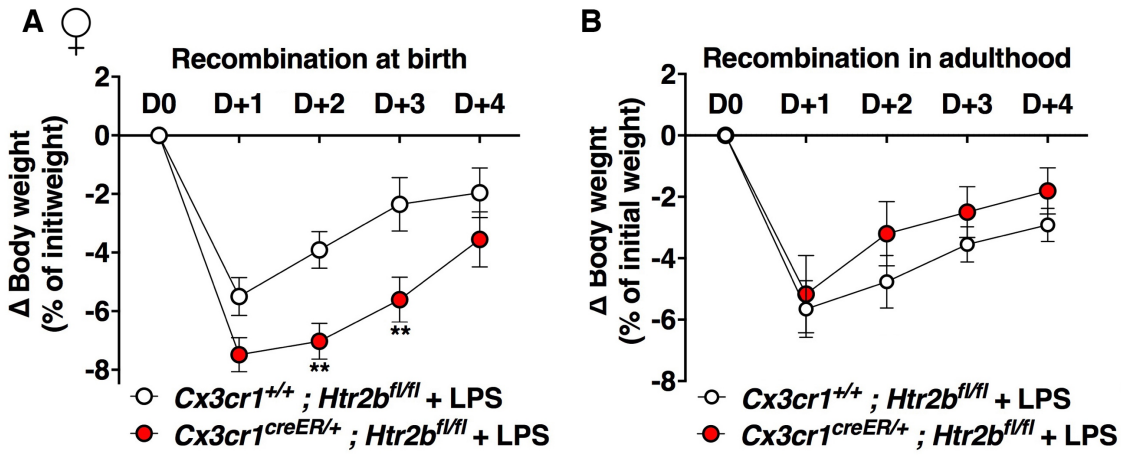


**Figure S8: Lack of *Htr2b* selectively in microglia since birth but not in adulthood is sufficient to enhance LPS-induced weight loss of adult females**. (**A**) *Htr2b* invalidation at birth: Time-course of weight variation after LPS injection in *Cx3cr1*$^{+/+}$*; Htr2b*$^{fl/fl}$ (white symbols) and *Cx3cr1*$^{CreERT2/+}$*; Htr2b*$^{fl/fl}$ (red symbols) female mice treated with tamoxifen at birth. Two-way ANOVA-RM showed an interaction between genotype and time ($F_{4,88}$ = 4.11, *p=0.0042*). Post hoc Bonferroni's multiple comparison between LPS-treated groups indicated a stronger weight loss in *Cx3cr1*$^{CreERT2/+}$*; Htr2b*$^{fl/fl}$ mice at D+2 and D+3 (**p=0.0076 and **p=0.0048, n=11 *Cx3cr1*$^{+/+}$*; Htr2b*$^{fl/fl}$ +LPS, and 13 *Cx3cr1*$^{CreERT2/+}$*; Htr2b*$^{fl/fl}$ +LPS). (**B**) *Htr2b* invalidation in adulthood: Time-course of weight variation after LPS injection in *Cx3cr1*$^{+/+}$*; Htr2b*$^{fl/fl}$ (white symbols) and *Cx3cr1*$^{CreERT2/+}$*; Htr2b*$^{fl/fl}$ (red symbols) female mice treated with tamoxifen in adulthood. Two-way ANOVA-RM showed no difference between genotypes after LPS injection. n=17 *Cx3cr1*$^{+/+}$*; Htr2b*$^{fl/fl}$ +LPS, and 15 *Cx3cr1*$^{CreERT2/+}$*; Htr2b*$^{fl/fl}$ +LPS.

**Table S1**

**Antibodies used for cytometry**

| Antibody/antigen | clone | label | company | reference | RRID |
|---|---|---|---|---|---|
| Fc block | 93 | none | Biolegend | 101320 | AB_312800 |
| CD11b | M1/70 | PE-Cy5 | Biolegend | 101209 | AB_312792 |
| CD11b | M1/70 | PE | AbD Serotec | MCA74PE | AB_321296 |
| Trem2 | 237920 | PE | R&D Systems | FAB17291P | AB_884528 |
| CD45 | 30-F11 | PE-Cy7 | Biolegend | 103114 | AB_312979 |

**Table S2**

**Primers used for RT-qPCR**

| Gene | Forward | Reverse | Fragment size |
|---|---|---|---|
| Spp1 | TGGCAGCTCAGAGGAGAAG | TTCTGTGGCGCAAGGAGATT | 101 |
| Ccl6 | CTTGTGGCTGTCCTTGGGTC | TACATGGGATCTGTGGGCA | 145 |
| Lipocalin 2 | ACAACCAGTTCGCCATGGTAT | AGCTCCTTGGTTCTTCCATACA | 88 |
| Ccl9 | ACCAGTGGTGGGTGTACCA | TTGTAGGTCCGTGGTTGTGA | 137 |
| Csf1 | TGCTCTAGCCGAGATGTGGT | CACTGCTAGGGGTGGCTT | 69 |
| Tnfrs11b | AGAAGCCACGCAAAAGTGTG | TCACTTTGGTCCCAGGCAAA | 131 |
| Tnf α | GAACTGGCAGAAGAGGCACT | AGGGTCTGGGCCATAGAACT | 203 |
| Il6 | CCGGAGAGGAGACTTCACAG | CAGAATTGCCATTGCACAAC | 133 |
| Il1β | GGACCCATATGAGCTGAAAGCT | TGTCGTTGCTTGGTTCTCCTT | 100 |
| Cyclophilin | CCATCGTGTCATCAAGGACTT | TTGCCATCCAGCCAGGAGGTC | 216 |
| Hexb | ACAAGAACCAGTAGCCGTCC | TGGTGAAAGTCCCGAAAGAGT | 106 |
| Fcrls | GTCGCTGGGGCACTGTATGT | GCACAGGCAGAGCTTCATCAA | 120 |

**Primers used to assess recombination at the *Htr2b* locus**

| Name | Sequence |
|---|---|
| F1 | CTAACATTTTTCATCCACATCTA |
| R1 | CCGCTCGAGCGGTGACTTC |
| F2 | TTGTTCAATGGCCGATCCCA |
| R2 | GGCATTCTGCACGCTTCAAA |
| R3 | ACTTTAATTGGGACTCGCTGAT |